BEST AVAILABLE IMAGES

Defective images within this document are accurate representations of the original documents submitted by the applicant.

Defects in the images may include (but are not limited to):

- BLACK BORDERS
- TEXT CUT OFF AT TOP, BOTTOM OR SIDES
- FADED TEXT
- ILLEGIBLE TEXT
- SKEWED/SLANTED IMAGES
- COLORED PHOTOS
- BLACK OR VERY BLACK AND WHITE DARK PHOTOS
- GRAY SCALE DOCUMENTS

IMAGES ARE BEST AVAILABLE COPY.

As rescanning documents *will not* correct images, please do not report the images to the Image Problem Mailbox.

Remarks

The Amendments

Claim 1 has been amended to recite that the claimed peptides are derived from *P. gingivalis* and to remove the prevention language. Claims 1 and 11 have been amended to remove the fragment/active site language. Claims 3, 4, 14, and 15 have been canceled. These amendments are made without prejudice to the prosecution of the un-amended subject matter in a continuing application. Claims 1 and 11 have been amended to change the "HagArep" term to "HArep1, HArep2, HArep3, and HArep4." This is not a narrowing amendment and is not made in response to a rejection. Rather, the amendment clarifies what peptides are being claimed. Support for the amendment appears in the specification at page 15, last paragraph. The amendments add no new matter. Applicants respectfully request entry of the amendments.

Rejection of Claims 1-4 and 11-15 Under 35 U.S.C. §112, first paragraph

Claims 1-4 and 11-15 stand rejected under 35 U.S.C. §112, first paragraph as allegedly lacking written description. Claims 3, 4, 14, and 15 have been canceled, the rejection is therefore moot as applied to these claims. Applicants respectfully traverse the rejection as it applies to claims 1-2 and 11-13.

The Office Action asserts that the specification lacks written description of proteases or peptides derived from organisms other than *P. gingivalis*. The Office Action furthermore asserts that the specification lacks written description for fragments or active sites of proteases or peptides. Applicants respectfully disagree with the Office; however, in order to expedite prosecution, Applicants have amended the claims to recite that the

McDONNELL BOEHNEN HULBERT & BERGHOFF
300 SOUTH WACKER DRIVE
CHICAGO, ILLINOIS 60606
TELEPHONE (312) 913-0001
FACSIMILE (312) 913-0002

proteases and peptides are *P. gingivalis* proteases and peptides. The claims have also been amended to delete the fragments and active site language.

Applicants respectfully request withdrawal of the rejection.

Rejection of Claims 1-4 and 11-15 Under 35 U.S.C. §112, first paragraph

Claims 1-4 and 11-15 stand rejected under 35 U.S.C. §112, first paragraph as allegedly lacking enablement. Claims 3, 4, 14, and 15 have been canceled, the rejection is therefore moot as applied to these claims. Applicants respectfully traverse the rejection as it applies to claims 1-2 and 11-13.

The Office Action asserts that Applicants' *in vitro* models do not reasonably correlate to the treatment or prevention of angioproliferative conditions. Initially, the Office Action asserts that the specification does not provide a "VEGF-induced" proliferation model. However, VEGF-induced proliferation models of *P. gingivalis* cysteine proteases are described in the attached declaration of Dr. Kozarov. See paragraphs 5-7. The VEGF-induced proliferation models demonstrate that *P. gingivalis* cysteine proteases treatment of VEGF-induced human endothelial cells results in proliferation inhibition. The models also demonstrate that *P. gingivalis* cysteine proteases not only disrupt the vasculature of the cells, especially the actively growing ones, but also trigger the cell death in the liberated cells thus eliminating them altogether. See paragraph 7.

The Applicants' previous response provided evidence that the VEGF-induced proliferation model was an art-recognized model for anti-angiogenic compounds. For example, the use of *in vitro* tests such as inhibition of VEGF-induced proliferation of endothelial cells assays have been shown to correlate with positive clinical results with,

McDONNELL BOEHNEN HULBERT & BERGHOFF
300 SOUTH WACKER DRIVE
CHICAGO, ILLINOIS 60606
TELEPHONE (312) 913-0001
FACSIMILE (312) 913-0002

for example, the anti-angioproliferative drug Avastin (also known as bevacizumab, anti-VEGF). *See* Presta *et al.*, J. Cancer Res. 57:4593 (1997) at page 4596, Col. 2, second full paragraph; ACS News "Drug shows promise against Advanced Colon Cancer" June, 2003 (copies attached). Additionally, Schlaeppi *et al.*, reported favorable results for anti-angiogenic compounds in VEGF-induced proliferation of endothelial cells assays. J Cancer Res Clin Oncol. 1999;125(6):336-42 (see page 340, second column, first full paragraph) (copy attached).

The Office Action asserts that evidence of enablement for a particular biological molecule known in the art (e.g., Avastin) does not extrapolate or reasonably predict the enablement of a completely distinct biological model because it has not been demonstrated that the currently claimed molecules have *in vivo* effects that correlate to their *in vitro* activity. However, Applicants are not presenting evidence of enablement of other biological molecules know in the art. Rather, Applicants are presenting evidence that the VEGF-induced proliferation inhibition assay is a correlating model for anti-angiogenic compounds such as *P. gingivalis* cysteine proteases.

Where a particular model is recognized in the art as reasonably correlating to a specific condition, it should be accepted as correlating by the Examiner. See MPEP §2164.01(c). A rigorous or an invariable exact correlation is not required. *See id.; Cross v. Iizuka*, 224 USPQ 739, 747). The art recognizes the VEGF-induced proliferation inhibition assay as a correlating model for anti-angiogenic compounds. Since the *P. gingivalis* cysteine proteases cause proliferation inhibition in the VEGF-induced proliferation assay, an art recognized model for anti-angiogenic compounds, one of skill in the art would be able to practice the invention without undue experimentation.

McDONNELL BOEHNEN HULBERT & BERGHOFF
300 SOUTH WACKER DRIVE
CHICAGO, ILLINOIS 60606
TELEPHONE (312) 913-0001
FACSIMILE (312) 913-0002

The declaration of Dr. Kozarov also presents data from apoptosis assays done with VEGF-induced primary human endothelial cells that were grown in the presence of VEGF. The data suggest that in addition to causing cell detachment from the substrate and total cell number reduction, *P. gingivalis* cysteine protease treatment results in a several-fold increase in apoptosis in treated primary endothelial cells. See paragraphs 2-4.

Additionally, the declaration of Dr. Kozarov provides ***in vivo*** evidence of the enablement of the claimed methods. For example, paragraphs 8-11 describe the effect of *P. gingivalis* cysteine proteases on lung and breast cancer murine animal models. Tumors treated with *P. gingivalis* cysteine proteases have large areas of necrosis indicating tumor tissue disintegration and endothelial destruction caused by compromised blood supply. See paragraph 10. In contrast, the control untreated tumors showed no sign of necrosis. See paragraph 10. Therefore, *P. gingivalis* cysteine proteases demonstrate anti-angioproliferative properties *in vivo* and *in vitro*. The recited *P. gingivalis* cysteine proteases have demonstrated *in vitro* anti-angioproliferative properties that correlate to *in vivo* properties, as described in the specification. One of skill in the art would be able to practice the invention, without an undue amount of experimentation. Therefore, the claims are enabled.

Applicants respectfully request withdrawal of the rejection.

Respectfully submitted,

Date: 3/1/04 By: _____

Lisa M.W. Hillman
Reg. No. 43,673

McDONNELL BOEHNEN HULBERT & BERGHOFF
300 SOUTH WACKER DRIVE
CHICAGO, ILLINOIS 60606
TELEPHONE (312) 913-0001
FACSIMILE (312) 913-0002

[CANCER RESEARCH 57, 4593–4599, October 15, 1997]

Humanization of an Anti-Vascular Endothelial Growth Factor Monoclonal Antibody for the Therapy of Solid Tumors and Other Disorders

Leonard G. Presta, Helen Chen, Shane J. O'Connor, Vanessa Chisholm, Y. Gloria Meng, Lynne Krummen, Marjorie Winkler, and Napoleone Ferrara[1]

Departments of Immunology, Process Sciences, Molecular Biology, Bioanalytical Technology and Cardiovascular Research, Genentech, Inc., South San Francisco, California 94080

ABSTRACT

Vascular endothelial growth factor (VEGF) is a major mediator of angiogenesis associated with tumors and other pathological conditions, including proliferative diabetic retinopathy and age-related macular degeneration. The murine anti-human VEGF monoclonal antibody (muMAb VEGF) A.4.6.1 has been shown to potently suppress angiogenesis and growth in a variety of human tumor cells lines transplanted in nude mice and also to inhibit neovascularization in a primate model of ischemic retinal disease. In this report, we describe the humanization of muMAb VEGF A.4.6.1, by site-directed mutagenesis of a human framework. Not only the residues involved in the six complementarity-determining regions but also several framework residues were changed from human to murine. Humanized anti-VEGF F(ab) and IgG1 variants bind VEGF with affinity very similar to that of the original murine antibody. Furthermore, recombinant humanized MAb VEGF inhibits VEGF-induced proliferation of endothelial cells *in vitro* and tumor growth *in vivo* with potency and efficacy very similar to those of muMAb VEGF A.4.6.1. Therefore, recombinant humanized MAb VEGF is suitable to test the hypothesis that inhibition of VEGF-induced angiogenesis is a valid strategy for the treatment of solid tumors and other disorders in humans.

INTRODUCTION

It is now well established that angiogenesis is implicated in the pathogenesis of a variety of disorders. These include solid tumors, intraocular neovascular syndromes such as proliferative retinopathies or AMD,[2] rheumatoid arthritis, and psoriasis (1, 2, 3). In the case of solid tumors, the neovascularization allows the tumor cells to acquire a growth advantage and proliferative autonomy compared to the normal cells. Accordingly, a correlation has been observed between density of microvessels in tumor sections and patient survival in breast cancer as well as in several other tumors (4–6).

The search for positive regulators of angiogenesis has yielded several candidates, including acidic fibroblast growth factor (FGF), bFGF, transforming growth factor α, transforming growth factor β, hepatocyte growth factor, tumor necrosis factor-α, angiogenin, interleukin 8, and others (1, 2). However, in spite of extensive research, there is still uncertainty as to their role as endogenous mediators of angiogenesis. The negative regulators thus far identified include thrombospondin (7), the M_r 16,000 NH_2-terminal fragment of prolactin (8), angiostatin (9), and endostatin (10).

Work done over the last several years has established the key role of VEGF in the regulation of normal and abnormal angiogenesis (11). The finding that the loss of even a single VEGF allele results in embryonic lethality points to an irreplaceable role played by this factor in the development and differentiation of the vascular system (11). Also, VEGF has been shown to be a key mediator of neovascularization associated with tumors and intraocular disorders (11). The VEGF mRNA is overexpressed by the majority of human tumors examined (12–16). In addition, the concentration of VEGF in eye fluids is highly correlated to the presence of active proliferation of blood vessels in patients with diabetic and other ischemia-related retinopathies (17). Furthermore, recent studies have demonstrated the localization of VEGF in choroidal neovascular membranes in patients affected by AMD (18).

The muMAb VEGF A.4.6.1 (19) has been used extensively to test the hypothesis that VEGF is a mediator of pathological angiogenesis *in vivo*. This high affinity MAb is able to recognize all VEGF isoforms (19) and has been shown to inhibit potently and reproducibly the growth of a variety of human tumor cell lines in nude mice (11, 20–23). Moreover, intraocular administration of muMAb VEGF A.4.6.1 resulted in virtually complete inhibition of iris neovascularization secondary to retinal ischemia in a primate model (24).

A major limitation in the use of murine antibodies in human therapy is the anti-globulin response (25, 26). Even chimeric molecules, where the variable (V) domains of rodent antibodies are fused to human constant (C) regions, are still capable of eliciting a significant immune response (27). A powerful approach to overcome these limitations in the clinical use of monoclonal antibodies is "humanization" of the murine antibody. This approach was pioneered by Jones *et al.* (28) and Riechman *et al.* (29), who first transplanted the CDRs of a murine antibody into human V domains antibody.

In the present article, we report on the humanization of muMAb VEGF A.4.6.1. Our strategy was to transfer the six CDRs, as defined by Kabat *et al.* (30), from muMAb VEGF A.4.6.1 to a consensus human framework used in previous humanizations (31–33). Seven framework residues in the humanized variable heavy (VH) domain and one framework residue in the humanized variable light (VL) domain were changed from human to murine to achieve binding equivalent to muMAb VEGF A.4.6.1. This humanized MAb is suitable for clinical trials to test the hypothesis that inhibition of VEGF action is an effective strategy for the treatment of cancer and other disorders in humans.

MATERIALS AND METHODS

Cloning of Murine Mab A.4.6.1 and Construction of Mouse-Human Chimeric Fab. Total RNA was isolated from hybridoma cells producing the anti-VEGF MAb A.4.6.1 using RNAsol (Tel-Test) and reverse-transcribed to cDNA using Oligo-dT primer and the SuperScript II system (Life Technologies, Inc., Gaithersburg, MD). Degenerate oligonucleotide primer pools, based of the NH_2-terminal amino acid sequences of the light and heavy chains of the antibody, were synthesized and used as forward primers. Reverse primers were based on framework 4 sequences obtained from murine light chain subgroup κV and heavy chain subgroup II (30). After PCR amplification, DNA fragments were ligated to a TA cloning vector (Invitrogen, San Diego, CA). Eight clones each of the light and

Received 5/27/97; accepted 8/16/97.

The costs of publication of this article were defrayed in part by the payment of page charges. This article must therefore be hereby marked *advertisement* in accordance with 18 U.S.C. Section 1734 solely to indicate this fact.

[1] To whom requests for reprints should be addressed, at Department of Cardiovascular Research, Genentech, Inc., 460 Point San Bruno Boulevard, South San Francisco, CA 94080. Phone: (415) 225-2968; Fax: (415) 225-6327; E-mail: Ferrara.Napoleone@gene.com.

[2] The abbreviations used are: AMD, age-related macular degeneration; bFGF, basic fibroblast growth factor; VEGF, vascular endothelial growth factor; MAb, monoclonal antibody; muMAb, murine MAb; rhuMAb, recombinant humanized MAb; CDR, complementarity-determining region.

heavy chains were sequenced. One clone with a consensus sequence for the light chain VL domain and one with a consensus sequence for the heavy chain VH domain were subcloned, respectively, into the pEMX1 vector containing the human CL and CH1 domains (31), thus generating a mouse-human chimeric F(ab). This chimeric F(ab) consisted of the entire murine A.4.6.1 VH domain fused to a human CH1 domain at amino acid SerH113, and the entire murine A.4.6.1 VL domain fused to a human CL domain at amino acid LysL107. Expression and purification of the chimeric F(ab) were identical to those of the humanized F(ab)s. The chimeric F(ab) was used as the standard in the binding assays.

Computer Graphics Models of Murine and Humanized F(ab)s. Sequences of the VL and VH domains (Fig. 1) were used to construct a computer graphics model of the murine A.4.6.1 VL-VH domains. This model was used to determine which framework residues should be incorporated into the humanized antibody. A model of the humanized F(ab) was also constructed to verify correct selection of murine framework residues. Construction of models was performed as described previously (32, 33).

Construction of Humanized F(ab)s. The plasmid pEMX1 used for mutagenesis and expression of F(ab)s in *Escherichia coli* has been described previously (31). Briefly, the plasmid contains a DNA fragment encoding a consensus human κ subgroup I light chain (VLκI-CL) and a consensus human subgroup III heavy chain (VHIII-CH1) and an alkaline phosphatase promoter. The use of the consensus sequences for VL and VH has been described previously (32).

To construct the first F(ab) variant of humanized A.4.6.1, F(ab)-1, site-directed mutagenesis (34) was performed on a deoxyuridine-containing template of pEMX1. The six CDRs were changed to the murine A.4.6.1 sequence; the residues included in each CDR were from the sequence-based CDR definitions (30). F(ab)-1, therefore, consisted of a complete human framework (VL κ subgroup I and VH subgroup III) with the six complete murine CDR sequences. Plasmids for all other F(ab) variants were constructed from the plasmid template of F(ab)-1. Plasmids were transformed into *E. coli* strain XL-1 Blue (Stratagene, San Diego, CA) for preparation of double- and single-stranded DNA. For each variant, DNA coding for light and heavy chains was completely sequenced using the dideoxynucleotide method (Sequenase; U.S. Biochemical Corp., Cleveland, OH). Plasmids were transformed into *E. coli* strain 16C9, a derivative of MM294, plated onto Luria broth plates containing 50 μg/ml carbenicillin, and a single colony selected for protein expression. The single colony was grown in 5 ml of Luria broth-100 μg/ml carbenicillin for 5–8 h at 37°C. The 5-ml culture was added to 500 ml of AP5–50 μg/ml carbenicillin and allowed to grow for 20 h in a 4-liter baffled shake flask at 30°C. AP5 media consists of 1.5 g of glucose, 11.0 g of Hycase SF, 0.6 g of yeast extract (certified), 0.19 g of $MgSO_4$ (anhydrous), 1.07 g of NH_4Cl, 3.73 g of KCl, 1.2 g of NaCl, 120 ml of 1 M triethanolamine, pH 7.4, to 1 liter of water and then sterile filtered through a 0.1-mm Sealkeen filter. Cells were harvested by centrifugation in a 1-liter centrifuge bottle at 3000 × *g*, and the supernatant was removed. After freezing for 1 h, the pellet was resuspended in 25 ml of cold 10 mM Tris, 1 mM EDTA, and 20% sucrose, pH 8.0. Two hundred fifty ml of 0.1 M benzamidine (Sigma Chemical Co., St. Louis, MO) was added to inhibit proteolysis. After gentle stirring on ice for 3 h, the sample was centrifuged at 40,000 × *g* for 15 min. The supernatant was then applied to a protein G-Sepharose CL-4B (Pharmacia Biotech, Inc., Uppsala, Sweden) column (0.5-ml bed volume) equilibrated with 10 mM Tris-1 mM EDTA, pH 7.5. The column was washed with 10 ml of 10 mM Tris-1 mM EDTA, pH 7.5, and eluted with 3 ml of 0.3 M glycine, pH 3.0, into 1.25 ml of 1 M Tris, pH 8.0. The F(ab) was then buffer exchanged into PBS using a Centricon-30 (Amicon, Beverly, MA) and concentrated to a final volume of 0.5 ml. SDS-PAGE gels of all F(ab)s were run to ascertain purity, and the molecular weight of each variant was verified by electrospray mass spectrometry.

Construction, Expression, and Purification of Chimeric and Humanized IgG Variants. For the generation of human IgG1 variants of chimeric (chIgG1) and humanized (rhuMAb VEGF) A.4.6.1, the appropriate murine or humanized VL and VH (F(ab)-12; Table 1) domains were subcloned into separate, previously described pRK vectors (35). The DNA coding for the entire light and the entire heavy chain of each variant was verified by dideoxynucleotide sequencing.

For transient expression of variants, heavy and light chain plasmids were cotransfected into human 293 cells (36) using a high efficiency procedure (37). Media were changed to serum free and harvested daily for up to 5 days. Antibodies were purified from the pooled supernatants using protein A-Sepharose CL-4B (Pharmacia). The eluted antibody was buffer exchanged into PBS using a Centricon-30 (Amicon), concentrated to 0.5 ml, sterile filtered using a Millex-GV (Millipore, Bedford, MA), and stored at 4°C.

For stable expression of the final humanized IgG1 variant (rhuMAb VEGF), Chinese hamster ovary (CHO) cells were transfected with dicistronic vectors designed to coexpress both heavy and light chains (38). Plasmids were introduced into DP12 cells, a proprietary derivative of the CHO-K1 DUX B11 cell line developed by L. Chasin (Columbia University, New York, NY), via lipofection and selected for growth in glycine/hypoxanthine/thymidine (GHT)-free medium (39). Approximately 20 unamplified clones were randomly chosen and reseeded into 96-well plates. Relative specific productivity of each colony was monitored using an ELISA to quantitate the full-length human IgG accumulated in each well after 3 days and a fluorescent dye, Calcien AM, as a surrogate marker of viable cell number per well. Based on these data, several unamplified clones were chosen for further amplification in the presence of increasing concentrations of methotrexate. Individual clones surviving at 10, 50, and 100 nM methotrexate were chosen and transferred to 96-well plates for productivity screening. One clone, which reproducibly exhibited high specific productivity, was expanded in T-flasks and used to inoculate a spinner

Table 1 *Binding of humanized anti-VEGF F(ab) variants to VEGF*[a]

Variant	Template	Changes[b]	Purpose	EC50 F(ab)-X EC_{50} chimeric F(ab)[c] Mean	SD	N
chim-F(ab)	Chimeric F(ab)		1.0			
F(ab)-1	Human FR		Straight CDR swap	>1350		2
F(ab)-2			Chimera light chain	>145		3
F(ab)-3			F(ab)-1 heavy chain F(ab)-1 light chain	2.6	0.1	2
F(ab)-4	F(ab)-1	ArgH71Leu AspH73Asn	Chimera heavy chain CDR-H2 conformation Framework	>295		3
F(ab)-5	F(ab)-4	LeuL46Val	VL-VH interface	80.9	6.5	2
F(ab)-6	F(ab)-5	LeuH78Ala	CDR-H1 conformation	36.4	4.2	2
F(ab)-7	F(ab)-5	IleH69Phe	CDR-H2 conformation	45.2	2.3	2
F(ab)-8	F(ab)-5	IleH69Phe LeuH78Ala	CDR-H2 conformation CDR-H1 conformation	9.6	0.9	4
F(ab)-9	F(ab)-8	GlyH49Ala	CDR-H2 conformation	>150		2
F(ab)-10	F(ab)-8	AsnH76Ser	Framework	6.4	1.2	4
F(ab)-11	F(ab)-10	LysH75Ala	Framework	3.3	0.4	2
F(ab)-12	F(ab)-10	ArgH94Lys	CDR-H3 conformation	1.6	0.6	4

[a] Anti-VEGF F(ab) variants were incubated with biotinylated VEGF and then transferred to ELISA plates coated with KDR-IgG (40).
[b] Murine residues are underlined; residue numbers are according to Kabat *et al.* (30).
[c] Mean and SD are the average of the ratios calculated for each of the independent assays; the EC_{50} for chimeric F(ab) was 0.049 ± 0.013 mg/ml (1.0 nM).

culture. After several passages, the suspension-adapted cells were used to inoculate production cultures in GHT-containing, serum-free media supplemented with various hormones and protein hydrolysates. Harvested cell culture fluid containing rhuMAb VEGF was purified using protein A-Sepharose CL-4B. The purity after this step was ~99%. Subsequent purification to homogeneity was carried out using an ion exchange chromatography step. The endotoxin content of the final purified antibody was <0.10 eu/mg.

F(ab) and IgG Quantitation. For quantitating F(ab) molecules, ELISA plates were coated with 2 μg/ml of goat anti-human IgG Fab (Organon Teknika, Durham, NC) in 50 mM carbonate buffer, pH 9.6, at 4°C overnight and blocked with PBS-0.5% BSA (blocking buffer) at room temperature for 1 h. Standards [0.78–50 ng/ml human F(ab)] were purchased from Chemicon (Temecula, CA). Serial dilutions of samples in PBS-0.5% BSA-0.05% polysorbate 20 (assay buffer) were incubated on the plates for 2 h. Bound F(ab) was detected using horseradish peroxidase-labeled goat anti-human IgG F(ab) (Organon Teknika), followed by 3,3',5,5'-tetramethylbenzidine (Kirkegaard & Perry Laboratories, Gaithersburg, MD) as the substrate. Plates were washed between steps. Absorbance was read at 450 nm on a V_{max} plate reader (Molecular Devices, Menlo Park, CA). The standard curve was fit using a four-parameter nonlinear regression curve-fitting program developed at Genentech. Data points that fell in the range of the standard curve were used for calculating the F(ab) concentrations of samples.

The concentration of full-length antibody was determined using goat anti-human IgG Fc (Cappel, Westchester, PA) for capture and horseradish peroxidase-labeled goat anti-human Fc (Cappel) for detection. Human IgG1 (Chemicon) was used as standard.

VEGF Binding Assays. For measuring the VEGF binding activity of F(ab)s, ELISA plates were coated with 2 μg/ml rabbit $F(ab')_2$ to human IgG Fc (Jackson ImmunoResearch, West Grove, PA) and blocked with blocking buffer (described above). Diluted conditioned medium containing 3 ng/ml of KDR-IgG (40) in blocking buffer were incubated on the plate for 1 h. Standards [6.9–440 ng/ml chimeric F(ab)] and 2-fold serial dilutions of samples were incubated with 2 nM biotinylated VEGF for 1 h in tubes. The solutions from the tubes were then transferred to the ELISA plates and incubated for 1 h. After washing, biotinylated VEGF bound to KDR was detected using horseradish peroxidase-labeled streptavidin (Zymed, South San Francisco, CA or Sigma) followed by 3,3',5,5'-tetramethylbenzidine as the substrate. Titration curves were fit with a four-parameter nonlinear regression curve-fitting program (KaleidaGraph; Synergy Software, Reading, PA). Concentrations of F(ab) variants corresponding to the midpoint absorbance of the titration curve of the standard were calculated and then divided by the concentration of the standard corresponding to the midpoint absorbance of the standard titration curve. Assays for full-length IgG were the same as for the F(ab)s except that the assay buffer contained 10% human serum.

BIAcore Biosensor Assays. VEGF binding of the humanized and chimeric F(ab)s were compared using a BIAcore biosensor (41). Concentrations of F(ab)s were determined by quantitative amino acid analysis. VEGF was coupled to a CM-5 biosensor chip through primary amine groups according to manufacturer's instructions (Pharmacia). Off-rate kinetics were measured by saturating the chip with F(ab) [35 μl of 2 μM F(ab) at a flow rate of 20 μl/min] and then switching to buffer (PBS-0.05% polysorbate 20). Data points from 0–4500 s were used for off-rate kinetic analysis. The dissociation rate constant (k_{off}) was obtained from the slope of the plot of $\ln(R0/R)$ *versus* time, where $R0$ is the signal at $t = 0$ and R is the signal at each time point.

On-rate kinetics were measured using 2-fold serial dilutions of F(ab) (0.0625–2 mM). The slope, K_s, was obtained from the plot of $\ln(-dR/dt)$ *versus* time for each F(ab) concentration using the BIAcore kinetics evaluation software as described in the Pharmacia Biosensor manual. R is the signal at time t. Data between 80 and 168, 148, 128, 114, 102, and 92 s were used for 0.0625, 0.125, 0.25, 0.5, 1, and 2 mM F(ab), respectively. The association rate constant (k_{on}) was obtained from the slope of the plot of K_s *versus* F(ab) concentration. At the end of each cycle, bound F(ab) was removed by injecting 5 μl of 50 mM HCl at a flow rate of 20 μl/min to regenerate the chip.

Endothelial Cell Growth Assay. Bovine adrenal cortex-derived capillary endothelial cells were cultured in the presence of low glucose DMEM (Life Technologies, Inc.) supplemented with 10% calf serum, 2 mM glutamine, and antibiotics (growth medium), essentially as described previously (42). For mitogenic assays, endothelial cells were seeded at a density of 6×10^3 cells/well in 6-well plates in growth medium. Either muMAb VEGF A.4.6.1 or rhuMAb VEGF was then added at concentrations ranging between 1 and 5000 ng/ml. After 2–3 h, purified *E. coli*-expressed $rhVEGF_{165}$ was added to a final concentration of 3 ng/ml. For specificity control, each antibody was added to endothelial cells at the concentration of 5000 ng/ml, either alone or in the presence of 2 ng/ml bFGF. After 5 or 6 days, cells were dissociated by exposure to trypsin, and duplicate wells were counted in a Coulter counter (Coulter Electronics, Hialeah, FL). The variation from the mean did not exceed 10%. Data were analyzed by a four-parameter curve fitting program (KaleidaGraph).

***In Vivo* Tumor Studies.** Human A673 rhabdomyosarcoma cells (American Type Culture Collection; CRL 1598) were cultured as described previously in DMEM/F12 supplemented with 10% fetal bovine serum, 2 mM glutamine, and antibiotics (20, 22). Female BALB/c nude mice, 6–10 weeks old, were injected s.c. with 2×10^6 tumor cells in the dorsal area in a volume of 200 μl. Animals were then treated with muMAb VEGF A.4.6.1, rhuMAb VEGF, or a control murine MAb directed against the gp120 protein. Both anti-VEGF MAbs were administered at the doses of 0.5 and 5 mg/kg; the control MAb was given at the dose of 5 mg/kg. Each MAb was administered twice weekly i.p. in a volume of 100 μl, starting 24 h after tumor cell inoculation. Each group consisted of 10 mice. Tumor size was determined at weekly intervals. Four weeks after tumor cell inoculation, animals were euthanized, and the tumors were removed and weighed. Statistical analysis was performed by ANOVA.

RESULTS

Humanization. The consensus sequence for the human heavy chain subgroup III and the light chain subgroup κ I were used as the framework for the humanization (Ref. 30; Fig. 1). This framework has been successfully used in the humanization of other murine antibodies (31, 32, 43, 44). All humanized variants were initially made and screened for binding as F(ab)s expressed in *E. coli*. Typical yields from 500-ml shake flasks were 0.1–0.4 mg F(ab).

Two definitions of CDR residues have been proposed. One is based on sequence hypervariability (30) and the other on crystal structures of F(ab)-antigen complexes (45). The sequence-based CDRs are larger than the structure-based CDRs, and the two definitions are in agreement except for CDR-H1: CDR-H1 includes residues H31–H35 according to the sequence-based definition, and residues H26–H32 according to the structure-based definition (light chain residue numbers are prefixed with L; heavy chain residue numbers are prefixed with H). We, therefore, defined CDR-H1 as a combination of the two, *i.e.*, including residues H26–H35. The other CDRs were defined using the sequence-based definition (30).

The chimeric F(ab) was used as the standard in the binding assays. In the initial variant, F(ab)-1, the CDR residues were transferred from the murine antibody to the human framework and, based on the models of the murine and humanized F(ab)s, the residue at position H49 (Ala in humans) was changed to the murine Gly. In addition, F(ab)s that consisted of the chimeric heavy chain/F(ab)-1 light chain [F(ab)-2] and F(ab)-1 heavy chain/chimeric light chain [F(ab)-3] were generated and tested for binding. F(ab)-1 exhibited a binding affinity greater than 1000-fold reduced from the chimeric F(ab) (Table 1). Comparing the binding affinities of F(ab)-2 and F(ab)-3 suggested that framework residues in the F(ab)-1 VH domain needed to be altered to increase binding.

Previous humanizations (31, 32, 43, 44) as well as studies of F(ab)-antigen crystal structures (45, 47) have shown that residues H71 and H73 can have a profound effect on binding, possibly by influencing the conformations of CDR-H1 and CDR-H2. Changing the human residues to their murine counterparts in F(ab)-4 improved binding by 4-fold (Table 1). Inspection of the models of the murine

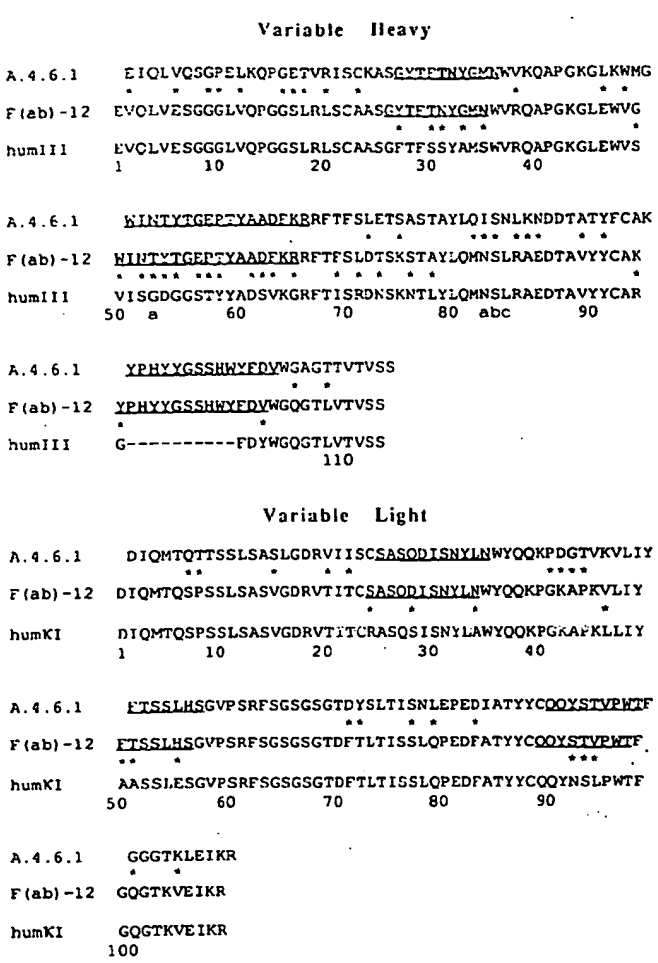

Fig. 1. Amino acid sequence of variable heavy and light domains of muMAbVEGF A.4.6.1, humanized F(ab) with optimal VEGF binding [F(ab)-12] and human consensus frameworks (*humIII*, heavy subgroup III; *humκI*, light κ subgroup I). *Asterisks*, differences between humanized F(ab)-12 and the murine MAb or between F(ab)-12 and the human framework. CDRs are *underlined*.

and humanized F(ab)s suggested that residue L46, buried at the VL-VH interface and interacting with CDR-H3 (Fig. 2), might also play a role either in determining the conformation of CDR-H3 and/or affecting the relationship of the VL and VH domains. When the murine Val was exchanged for the human Leu at L46 [F(ab)-5], the binding affinity increased by almost 4-fold (Table 1). Three other buried framework residues were evaluated based on the molecular models: H49, H69, and H78. Position H69 may affect the conformation of CDR-H2, whereas position H78 may affect the conformation of CDR-H1 (Fig. 2). When each was individually changed from the human to murine counterpart, the binding improved by 2-fold in each case [F(ab)-6 and F(ab)-7; Table 1]. When both were simultaneously changed, the improvement in binding was 8-fold [F(ab)-8; Table 1]. Residue H49 was originally included as the murine Gly; when changed to the human consensus counterpart Ala, the binding was reduced by 15-fold [F(ab)-9; Table 1].

We have found during previous humanizations that residues in a framework loop, FR-3 (30) adjacent to CDR-H1 and CDR-H2, can affect binding (44). In F(ab)-10 and F(ab)-11, two residues in this loop were changed to their murine counterparts: AsnH76 to murine Ser [F(ab)-10] and LysH75 to murine Ala [F(ab)-11]. Both effected a relatively small improvement in binding (Table 1). Finally, at position H94, human and murine sequences most often have an Arg (30). In F(ab)-12, this Arg was replaced by the rare Lys found in the murine antibody (Fig. 1), and this resulted in binding that was less than 2-fold from the chimeric F(ab) (Table 1). F(ab)-12 was also compared to the chimeric F(ab) using the BIAcore system (Pharmacia). Using this technique, the K_d of the humanized F(ab)-12 was 2-fold weaker than that of the chimeric F(ab) due to both a slower k_{on} and faster k_{off} (Table 2).

Full-length MAbs were constructed by fusing the VL and VH domains of the chimeric F(ab) and variant F(ab)-12 to the constant domains of human κ light chain and human IgG1 heavy chain. The full-length 12-IgG1 [F(ab)-12 fused to human IgG1] exhibited binding that was 1.7-fold weaker than the chimeric IgG1 (Table 3). Both 12-IgG1 and the chimeric IgG1 bound slightly less well than the original muMAb VEGF A.4.6.1 (Table 3).

Biological Studies. rhuMAb VEGF and muMAb VEGF A.4.6.1 were compared for their ability to inhibit bovine capillary endothelial cell proliferation in response to a near maximally effective concentration of $VEGF_{165}$ (3 ng/ml). In several experiments, the two MAbs were found to be essentially equivalent, both in potency and efficacy. The ED_{50}s were, respectively, 50 ± 5 and 48 ± 8 ng/ml (~0.3 nM). In both cases, 90% inhibition was achieved at the concentration of 500 ng/ml (~3 nM). Fig. 3 illustrates a representative experiment. Neither muMAb VEGF A.4.6.1 nor rhuMAb VEGF had any effect on basal or bFGF-stimulated proliferation of capillary endothelial cells (data not shown), confirming that the inhibition is specific for VEGF.

To determine whether similar findings could be obtained also in an *in vivo* system, we compared the two antibodies for their ability to suppress the growth of human A673 rhabdomyosarcoma cells in nude mice. Previous studies have shown that muMAb VEGF A.4.6.1 has a dramatic inhibitory effect in this tumor model (20, 22). As shown in Fig. 4, at both doses tested (0.5 and 5 mg/kg), the two antibodies markedly suppressed tumor growth as assessed by tumor weight measurements 4 weeks after cell inoculation. The decreases in tumor weight compared to the control group were, respectively, 85 and 93% at each dose in the animals treated with muMAb VEGF A.4.6.1 *versus* 90 and 95% in those treated with rhuMAb VEGF. Similar results were obtained with the breast carcinoma cell line MDA-MB 435 (data not shown).

DISCUSSION

The murine MAb A.4.6.1, directed against human VEGF (42), was humanized using the same consensus frameworks for the light and heavy chains used in previous humanizations (31, 32, 43, 44), *i.e.*, VκI and VHIII (30). Simply transferring the CDRs from the murine antibody to the human framework resulted in a F(ab) that exhibited binding to VEGF reduced by over 1000-fold compared to the parent murine antibody. Seven non-CDR, framework residues in the VH domain and one in the VL domain were altered from human to murine to achieve binding equivalent to the parent murine antibody.

In the VH domain, residues at positions H49, H69, H71, and H78 are buried or partially buried and probably effect binding by influencing the conformation of the CDR loops. Residues H73 and H76 should be solvent exposed (Fig. 2) and hence may interact directly with the VEGF; these two residues are in a non-CDR loop adjacent to CDRs H1 and H2 and have been shown to play a role in binding in previous humanizations (31, 32, 44). The requirement for lysine at position H94 was surprising given that this residue is arginine in the human framework (Fig. 1). In some crystal structures of F(ab)s, ArgH94 forms a hydrogen-bonded salt-bridge with

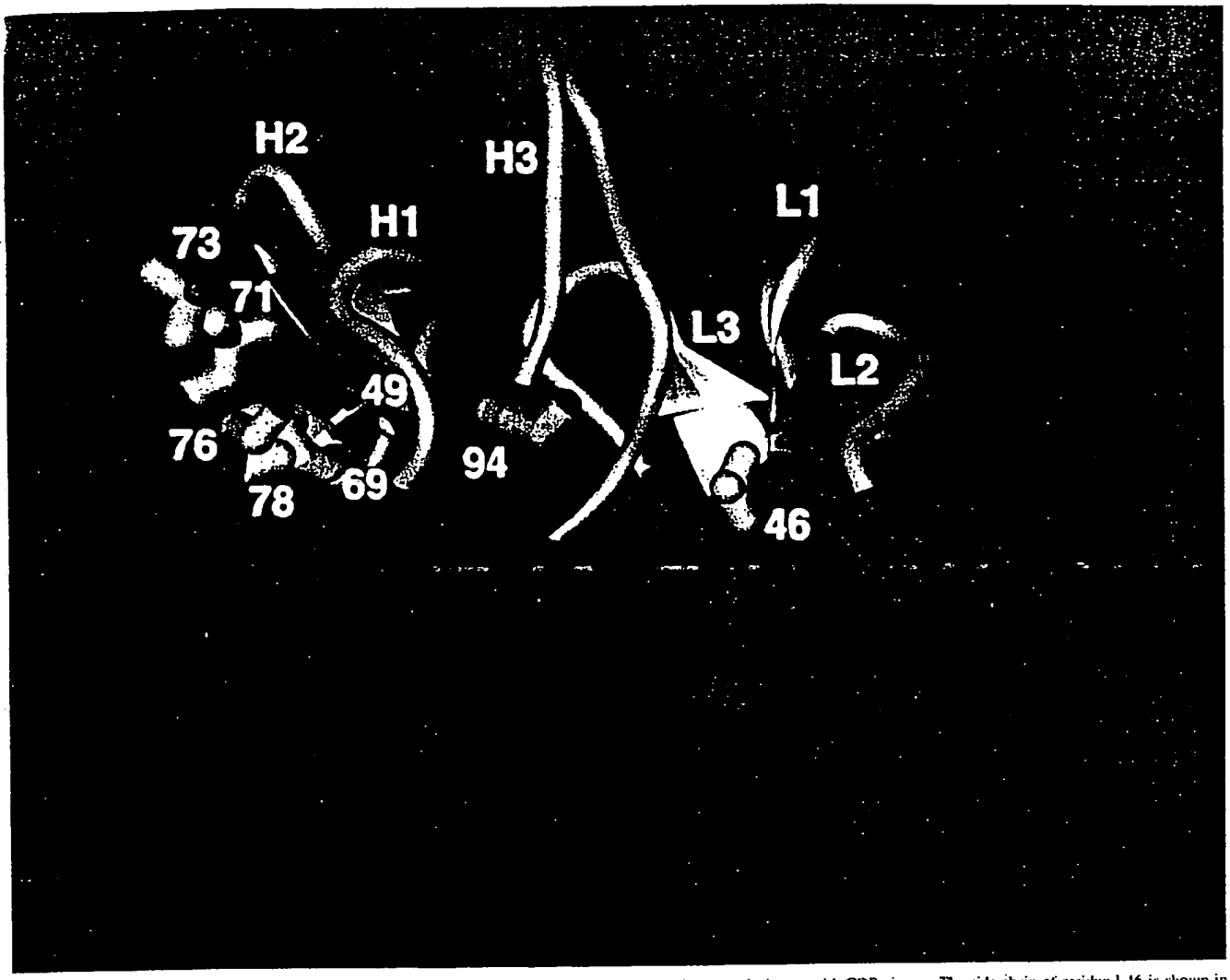

Fig. 2. Ribbon diagram of the model of humanized F(ab)-12 VL and VH domains. VL domain is shown in *brown* with CDRs in *tan*. The side chain of residue L46 is shown in *yellow*. VH domain is shown in *purple* with CDRs in *pink*. Side chains of VH residues changed from human to murine are shown in *yellow*.

Table 2 *Binding of anti-VEGF F(ab) variants to VEGF using the BIAcore system*[a]

Variant	Amount of (Fab) bound (RU)	k_{off} (s^{-1})	k_{on} ($M^{-1}s^{-1}$)	K_d (nM)
chim-F(ab)[b]	4250	5.9×10^{-5}	6.5×10^{4}	0.91
F(ab)-12	3740	6.3×10^{-5}	3.5×10^{4}	1.8

[a] The amount of F(ab) bound, in resonance units (RU), was measured using a BIAcore system when 2 μg F(ab) was injected onto a chip containing 2480 RU of immobilized VEGF. Off-rate kinetics (k_{off}) were measured by saturating the chip with F(ab) and then monitoring dissociation after switching to buffer. On-rate kinetics (k_{on}) were measured using 2-fold serial dilutions of F(ab). K_d, the equilibrium dissociation constant, was calculated as k_{off}/k_{on}.

[b] chim-F(ab) is a chimeric F(ab) with murine VL and VH domains fused to human CL and CH1 heavy domains.

AspH101 (33, 48). Substitution of lysine for arginine might conceivably alter this salt-bridge and perturb the conformation of CDR-H3.

In the VL domain, only one framework residue had to be changed to murine to optimize the humanization. Position L46 is at the VL-VH interface, where it is buried and interacts directly with CDR-H3 (Fig. 2). The requirement for murine valine (as opposed to human leucine) implies that this residue plays an important role in the conformation of CDR-H3. The necessity of retaining LysH94 in VH, which is also adjacent to CDR-H3, suggests that CDR-H3 plays a major role in the binding of the antibody to VEGF.

The humanized version with optimal binding, 12-IgG1, exhibited only a 2-fold reduction in binding compared to the parent murine antibody (Table 3). An analysis of the binding kinetics of the humanized and chimeric F(ab)s showed that both had similar off-rates but that the humanized F(ab) had a 2-fold slower on-rate (Table 2), which accounts for the 2-fold reduction in binding. However, this modest reduction in on-rate did not result in any decreased ability to antagonize VEGF bioactivity. The two anti-

Table 3 *Binding of anti-VEGF IgG variants to VEGF*[a]

Variant	IgG1/chIgG1[b] Mean	SD	N
chIgG1	1.0		2
murIgG1[c]	0.759	0.001	2
12-IgG1[d]	1.71	0.03	2

[a] Anti-VEGF IgG variants were incubated with biotinylated VEGF and then transferred to ELISA plates coated with KDR-IgG (40).

[b] chIgG1 is chimeric IgG1 with murine VL and VH domains fused to human CL and IgG1 heavy chains; the EC_{50} for chIgG1 was 0.113 ± 0.013 μg/ml (0.75 nM).

[c] murIgG1 is muMAb VEGF-A.4.6.1 purified from ascites.

[d] 12-IgG1 is F(ab)-12 VL and VH domains fused to human CL and IgG1 heavy chains.

bodies had essentially identical activity, both in an endothelial cell proliferation assay and in an *in vivo* tumor model.

Interestingly, an alternative approach using monovalent phage display has been also applied to the humanization of muMAb VEGF A.4.6.1. (49). Random mutagenesis of framework residues resulted in selection of variants with significantly improved affinity compared to the initial humanized MAb with no framework changes. However; the best variant obtained by this method had a less complete restoration of the binding affinity of muMAb VEGF A.4.6.1 compared to that reported in this study (49). Clearly, this does not rule out the possibility that other applications of phage display, such as affinity maturation of the CDRs (50), may result in variants with even higher affinity.

In conclusion, protein engineering techniques resulted in virtually complete acquisition by a human immunoglobulin framework of the binding properties and biological activities of a high-affinity murine anti-VEGF MAb. In view of the nearly ubiquitous up-regulation of VEGF mRNA in human tumors (12–16) and the ability of muMAb VEGF A.4.6.1 to inhibit the *in vivo* growth of a broad spectrum of tumor cell lines (20–23), VEGF is a major target of anticancer therapy. Clinical trials using rhuMAb VEGF should allow us to test the hypothesis that inhibition of VEGF-mediated angiogenesis is an effective strategy for the treatment of several solid tumors in humans. Such trials are already under way. Other important clinical applications of rhuMAb VEGF include the prevention of blindness secondary to proliferative diabetic retinopathy (17) or AMD (18). Clearly, the success of the humanization can be ultimately judged by the degree of anti-human globulin response and and by the clinical response in patients. However, the recent report of a Phase II study where rhuMAb HER2, a humanized MAb with the same framework as rhuMAb VEGF, did not induce any anti-globulin response in breast cancer patients and also demonstrated clinical efficacy (51), makes one optimistic. The results of this (51) as well as other (52) trials raise hope that, after many disappointing results (53), progress in antibody technology, coupled with selection of better targets, will bring therapy with MAbs closer to fulfilling its promises.

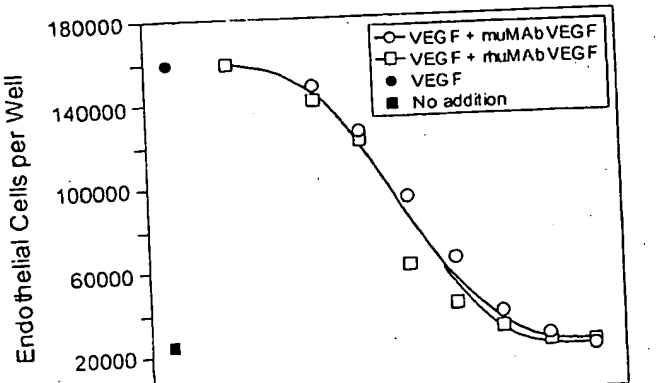

Fig. 3. Inhibition of VEGF-induced mitogenesis. Bovine adrenal cortex-derived capillary endothelial cells were seeded at the density of 6×10^4 cells/well in six-well plates, as described in "Materials and Methods." Either muMAb VEGF A.4.6.1 or rhuMAb VEGF (IgG1) was added at the indicated concentrations. After 2–3 h, $rhVEGF_{165}$ was added at the final concentration of 3 ng/ml. After 5 or 6 days, cells were trypsinized and counted. Values shown are means of duplicate determinations. The variation from the mean did not exceed 10%.

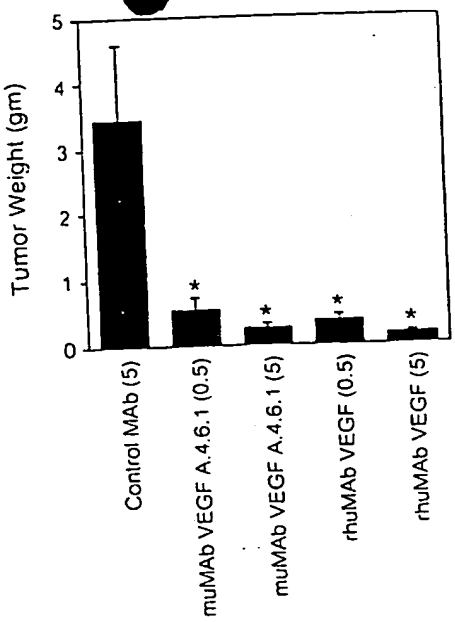

Fig. 4. Inhibition of tumor growth *in vivo*. A673 rhabdomyosarcoma cells were injected in BALB/c nude mice at the density of 2×10^6 per mouse. Starting 24 h after tumor cell inoculation, animals were injected with a control MAb, muMAb VEGF A.4.6.1, or rhuMab VEGF (IgG1) twice weekly, i.p. The dose of the control MAb was 5 mg/kg; the anti-VEGF MAbs were given at 0.5 or 5 mg/kg, as indicated ($n = 10$). Four weeks after tumor cell injection, animals were euthanized, and tumors were removed and weighed. *, significant difference when compared to the control group by ANOVA ($P < 0.05$).

ACKNOWLEDGMENTS

We thank K. Garcia for performing the VEGF binding ELISA, W. Henzel for protein microsequencing, A. Padua for amino acid analysis, J. Bourell for mass spectrometry, and J. Silva for animal studies. We are grateful to the DNA synthesis and the DNA sequencing groups at Genentech. We also thank C. Adams, J. Kim, B. Fendly, B. Keyt, and M. Beresini for helpful comments and advice.

REFERENCES

1. Folkman, J., and Shing, Y. Angiogenesis. J. Biol. Chem., *267:* 10931–10934, 1992.
2. Klagsbrun, M., and D'Amore, P. A. Regulators of angiogenesis. Annu. Rev. Physiol., *53:* 217–239, 1991.
3. Garner, A. Vascular diseases. *In:* A. Garner and G. K. Klintworth (eds.), Pathobiology of Ocular Disease. A Dynamic Approach, Ed. 2, pp. 1625–1710. New York: Marcel Dekker, 1994.
4. Weidner, N., Semple, P., Welch, W., and Folkman, J. Tumor angiogenesis and metastasis. Correlation in invasive breast carcinoma. N. Engl. J. Med., *324:* 1–6, 1991.
5. Horak, E. R., Leek, R., Klenk, N., Lejeune, S., Smith, K., Stuart, M., Greenall, M., and Harris, A. Quantitative angiogenesis assessed by anti-PECAM antibodies; correlation with node metastasis and survival in breast cancer. Lancet, *340:* 1120–1124, 1992.
6. Macchiarini, P., Fontanini, G., Hardin, M. J., Squartini, F., and Angeletti, C. A. Relation of neovascularization to metastasis of non-small cell lung carcinoma. Lancet, *340:* 145–146, 1992.
7. Good, D., Polverini, P., Rastinejad, F., Beau, M., Lemons, R., Frazier, W., and Bouck, N. A tumor suppressor-dependent inhibitor of angiogenesis is immunologically and functionally indistinguishable from a fragment of thrombospondin. Proc. Natl. Acad. Sci. USA, *87:* 6624–6628, 1990.
8. Clapp, C., Martial, J. A., Guzman, R. C., Rentier-Delrue, F., and Weiner, R. I. The 16-kilodalton N-terminal fragment of human prolactin is a potent inhibitor of angiogenesis. Endocrinology, *133:* 1292–1299, 1993.
9. O'Reilly, M. S., Holmgren, L., Shing, Y., Chen, C., Rosenthal, R. A., Moseni, M., Lane, W. S., Cao, Y., Sage, E. H., and Folkman, J. Angiostatin. A novel angiogenesis inhibitor that mediates the suppression of metastasis by a Lewis lung carcinoma. Cell, *79:* 315–328, 1994.
10. O'Reilly, M. S., Boehm, T., Shing, Y., Fukai, N., Vasios, G., Lane, W. S., Flynn, E., Birkhead, J. R., Olsen, B. R., and Folkman, J. Endostatin. An endogenous inhibitor of angiogenesis and tumor growth. Cell, *88:* 277–285, 1996.
11. Ferrara, N., and Davis Smyth, T. The biology of vascular endothelial growth factor. Endocr. Rev., *18:* 4–25, 1997.

12. Berkman, R. A., Merrill, M. J., Reinhold, W. C., Monacci, W. T., Saxena, A., Clark, W. C., Robertson, J. T., Ali, I. U., and Oldfield, E. H. Expression of the vascular permeability/vascular endothelial growth factor gene in central nervous system neoplasms. J. Clin. Invest., *91:* 153–159, 1993.
13. Brown, L. F., Berse, B., Jackman, R. W., Guidi, A. J., Dvorak, H. F., Senger, D. R., Connolly, J. L., and Schnitt, S. J. Expression of vascular permeability factor (vascular endothelial growth factor) and its receptors in breast cancer. Hum. Pathol., *26:* 86–91, 1995.
14. Brown, L. F., Berse, B., Jackman, R. W., Tognazzi, K., Manseau, E. J., Senger, D. R., and Dvorak, H. F. Expression of vascular permeability factor (vascular endothelial growth factor) and its receptors in adenocarcinomas of the gastrointestinal tract. Cancer Res., *53:* 4727–4735, 1993.
15. Matteri, J., Koomagi, R., and Volm, M. Association of vascular endothelial growth factor expression with intratumoral microvessel density and tumour cell proliferation in human epidermoid lung carcinoma. Br. J. Cancer, *73:* 931–934, 1996.
16. Dvorak, H. F., Brown, L. F., Detmar, M., and Dvorak, A. M. Vascular permeability factor/vascular endothelial growth factor, microvascular permeability and angiogenesis. Am. J. Pathol., *146:* 1029–1039, 1995.
17. Aiello, L. P., Avery, R., Arrigg, R., Keyt, B., Jampel, H., Shah, S., Pasquale, L., Thieme, H., Iwamoto, M., Park, J. E., Nguyen, H., Aiello, L. M., Ferrara, N., and King, G. L. Vascular endothelial growth factor in ocular fluid of patients with diabetic retinopathy and other retinal disorders. N. Engl. J. Med., *331:* 1480–1487, 1994.
18. Lopez, P. F., Sippy, B. D., Lambert, H. M., Thach, A. B., and Hinton, D. R. Transdifferentiated retinal pigment epithelial cells are immunoreactive for vascular endothelial growth factor in surgically excised age-related macular degeneration-related choroidal neovascular membranes. Invest. Ophthalmol. Visual Sci., *37:* 855–868, 1996.
19. Kim, K. J., Li, B., Houck, K., Winer, J., and Ferrara, N. The vascular endothelial growth factor proteins: identification of biologically relevant regions by neutralizing monoclonal antibodies. Growth Factors, *7:* 53–64, 1992.
20. Kim, K. J., Li, B., Winer, J., Armanini, M., Gillett, N., Phillips, H. S., and Ferrara, N. Inhibition of vascular endothelial growth factor-induced angiogenesis suppresses tumour growth *in vivo*. Nature (Lond.), *362:* 841–844, 1993.
21. Warren, R. S., Yuan, H., Matli, M. R., Gillett, N. A., and Ferrara, N. Regulation by vascular endothelial growth factor of human colon cancer tumorigenesis in a mouse model of experimental liver metastasis. J. Clin. Invest., *95:* 1789–1797, 1995.
22. Borgström, P., Hillan, K. J., Sriramarao, P., and Ferrara, N. Complete inhibition of angiogenesis and growth of microtumors by anti-vascular endothelial growth factor neutralizing antibodies. Novel concepts of angiostatic therapy from intravital videomicroscopy. Cancer Res., *56:* 4032–4039, 1996.
23. Melnyk, O., Schuman, M. A., and Kim, K. J. Vascular endothelial growth factor promotes tumor dissemination by a mechanism distinct from its effect on primary tumor growth. Cancer Res., *56:* 921–924, 1996.
24. Adamis, A. P., Shima, D. T., Tolentino, M., Gragoudas, E., Ferrara, N., Folkman, J., D'Amore, P. A., and Miller, J. W. Inhibition of VEGF prevents retinal ischemia-associated iris neovascularization in a primate. Arch. Ophthalmol., *114:* 66–71, 1996.
25. Miller, R. A., Oseroff, A. R., Stratte, P. T., and Levy, R. Monoclonal antibody therapeutic trials in seven patients with T-cell lymphoma. Blood, *62:* 988–995, 1983.
26. Schroff, R. W., Foon, K. A., Beatty, S. M., Odham, R. K., and Morgan, A. C., Jr. Human anti-murine immunoglobulin response in patients receiving monoclonal antibody therapy. Cancer Res., *45:* 879–885, 1985.
27. Neuberger, M. S., Williams, G. T., Mitchell, E. B., Jouhal, S. S., Flanagan, J. G., and Rabbits, T. H. A hapten-specific chimaeric IgE antibody with human physiological effector function. Nature (Lond.), *314:* 268–270, 1985.
28. Jones, P. T., Dear, P. H., Foote, J., Neuberger, M. S., and Winter, G. Replacing the complementarity-determining regions in a human antibody with those from a mouse. Nature (Lond.), *321:* 522–525, 1986.
29. Riechmann, L., Clark, M., Waldmann, H., and Winter, G. Reshaping human antibodies for therapy. Nature (Lond.), *332:* 323–327, 1988.
30. Kabat, E. A., Wu, T. T., Perry, H. M., Gottesmann, K. S., and Foeller, C. Sequences of proteins of immunological interest, Ed. 5. Public Health Service, National Institutes of Health, Bethesda, MD, 1991.
31. Werther, W. A., Gonzalez, T. N., O'Connor, S. J., McCabe, S., Chan, B., Hotaling, T., Champe, M., Fox, J. A., Jardieu, P. M., Berman, P. W., and Presta, L. G. Humanization of an anti-lymphocyte function-associated antigen (LFA)-1 monoclonal antibody and reengineering of the humanized antibody for binding to rhesus LFA-1. J. Immunol., *157:* 4986–4995, 1996.
32. Carter, P., Presta, L., Gorman, C. M., Ridgway, J. B. B., Henner, D., Wong, W. L. T., Rowland, A. M., Kotts, C., Carver, M. E., and Shepard, H. M. Humanization of an anti-p185HER2 antibody for human cancer therapy. Proc. Natl. Acad. Sci. USA, *89:* 4285–4289, 1992.
33. Eigenbrot, C., Randal, M., Presta, L., and Kossiakoff, A. A. X-ray structures of the antigen-binding domains from three variants of humanized anti-p185HER2 antibody 4D5 and comparison with molecular modeling. J. Mol. Biol., *229:* 969–995, 1993.
34. Kunkel, T. A. Rapid and efficient site-specific mutagenesis without phenotypic selection. Proc. Natl. Acad. Sci. USA, *82:* 488–492, 1985.
35. Eaton, D. L., Wood, W. I., Eaton, D., Hass, P. E., Hollingshead, P., Wion, K., Mather, J., Lawn, R. M., Vehar, G. A., and Gorman, C. Construction, and characterization of an active factor VIII variant lacking the central one-third of the molecule. Biochemistry, *25:* 8343–8347, 1986.
36. Graham, F. L., Smiley, J., Russell, W. C., and Nairn, R. Characteristics of a human cell line transformed by DNA from human adenovirus type 5. J. Gen. Virol., *36:* 59–74, 1977.
37. Gorman, C. M., Gies, D. R., and McCray, G. Transient production of proteins using an adenovirus transformed cell line. DNA Prot. Eng. Tech., *2:* 3–10, 1990.
38. Lucas, B. K., Giere, L. M., DeMarco, R. A., Chisholm, V., and Crowley, C. W. High-level production of recombinant proteins in CHO cells using a dicistronic DHFR intron expression vector. Nucleic Acids Res., *24:* 1774–1779, 1996.
39. Chisholm, V. High efficiency gene transfer in mammalian cells. *In:* D. M. Glover and B. D. Hames (eds.), DNA Cloning 4. Mammalian systems, pp. 1–41. Oxford: Oxford University Press, 1996.
40. Park, J. E., Chen, H., Winer, J., Houck, K. A., and Ferrara, N. Placenta growth factor. Potentiation of VEGF bioactivity, *in vitro* and *in vivo*, and high affinity binding to Flt-1 but not to Flk-1/KDR. J. Biol. Chem., *269:* 25646–25645, 1994.
41. Karlsson, R., Roos, H., Fagerstam, L., and Persson, B. Kinetic and concentration analysis using BIA technology. Methods: A Companion to Methods in Enzymology, Vol. 6, pp. 97–108, 1994.
42. Leung, D. W., Cachianes, G., Kuang, W-J., Goeddel, D. V., and Ferrara, N. Vascular endothelial growth factor is a secreted angiogenic mitogen. Science (Washington DC), *246:* 1306–1309, 1989.
43. Presta, L. G., Lahr, S. J., Shields, R. L., Porter, J. P., Gorman, C. M., Fendly, B. M., and Jardieu, P. M. Humanization of an antibody directed against IgE. J. Immunol., *151:* 2623–2632, 1993.
44. Eigenbrot, C., Gonzalez, T., Mayeda, J., Carter, P., Werther, W., Hotaling, T., Fox, J., and Kessler, J. X-ray structures of fragments from binding and nonbinding versions of a humanized anti-CD18 antibody: structural indications of the key role of VH residues 59 to 65. Proteins, *18:* 49–62, 1994.
45. Chothia, C., Lesk, A. M., Tramontano, A., Levitt, M., Smith-Gill, S. J., Air, G., Sheriff, S., Padlan, E. A., Davies, D., Tulip, W. R., Colman, P. M., Spinelli, S., Alzari, P. M., and Poljak, R. J. Conformations of immunoglobulin hypervariable regions. Nature (Lond.), *342:* 877–883, 1989.
46. Xiang, J., Sha, Y., Jia, Z., Prasad, L., and Delbaere, L. T. Framework residues 71 and 93 of the chimeric B72.3 antibody are major determinants of the conformation of heavy-chain hypervariable loops. J. Mol. Biol., *253:* 385–390, 1995.
47. Tramontano, A., Chothia, C., and Lesk, A. M. Framework residue 71 is a major determinant of the position and conformation of the second hypervariable region in the VH domains of immunoglobulins. J. Mol. Biol., *215:* 175–182, 1990.
48. Fischmann, T. O., Bentley, G. A., Bhat, T. N., Boulot, G., Mariuzza, R. A., Phillips, S. E. V., Tello, D., and Poljak, R. J. Crystallographic refinement of the three-dimensional structure of the FabD1.3-lysozyme complex at 2.5-Å resolution. J. Biol. Chem., *266:* 12915–12920, 1994.
49. Baca, M., Presta, L. G., O'Connor, S. J., and Wells, J. A. Antibody humanization using monovalent phage display. J. Biol. Chem., *272:* 10678–10684, 1997.
50. Barbas, C. F., III. Selection and evolution of high-affinity anti-viral antibodies. Trends Biotechnol., *14:* 230–234, 1996.
51. Baselga, J., Tripathy, D., Mendelshon, J., Baughman, S., Benz, C. C., Dantis, L., Sklarin, N. T., Deidman, A. D., Hudis, C. A., Moore, J., Rosen, P. P., Twaddel, T., Henderson, I. C., and Norton, L. Phase II study of weekly intravenous recombinant humanized anti-p185^{HER2} monoclonal antibody in patients with HER2/neu overexpressing metastatic breast cancer. J. Clin. Oncol., *14:* 737–744, 1996.
52. von Mehren, M., and Weiner, L. M. Monoclonal antibody-based therapy. Curr. Opin. Oncol., *8:* 493–498, 1996.
53. Riethmuller, G., Schneider-Gadicke, E., and Johnson, J. P. Monoclonal antibodies in cancer therapy. Curr. Opin. Immunol., *5:* 732–739, 1993.

ACS news:

Drug Shows Promise Against Advanced Colon Cancer

Targets Tumor's Blood Supply

June 04, 2003 02:37:23 PM PST, ACS News Center

An experimental drug that targets the blood supply of tumors can help people with advanced colorectal cancer live longer, according to research presented at a recent oncology meeting. The findings give hope to scientists who have been pursuing this avenue of treatment known as antiangiogenesis therapy for years, without success.

"Our study offers important proof of the philosophy that targeting a tumor's blood supply can, in fact, inhibit the tumor's ability to proliferate," said lead investigator Herbert Hurwitz, MD, of Duke University Medical Center, in a statement.

Hurwitz and his colleagues studied more than 800 people with metastatic colorectal cancer (cancer that had spread to other parts of the body). Half the group received standard chemotherapy for their disease, while the others were treated with standard chemotherapy plus the experimental drug bevacizumab (Avastin), made by Genentech.

Patients Survived Longer

Patients receiving Avastin lived about five months longer than patients on the standard regimen alone, Hurwitz reported at the annual meeting of the American Society of Clinical Oncology in Chicago. In addition, more of the Avastin patients saw their tumors shrink, and it took longer for their tumors to resume growing.

Side effects reported in the study were not severe, the researchers said. About 11% of patients developed high blood pressure while taking Avastin, but the condition was manageable with standard medications.

The results are "extremely significant," said Durado Brooks, MD, director of prostate and colorectal cancer for the American Cancer Society. Advanced disease is very aggressive, he said, and extremely hard to treat with existing chemotherapy regimens.

"Because the outcomes are so poor with advanced disease, it's marvelous to have a new arrow in our quiver," Brooks said.

Screening Still Critical Until There's a Cure

However, he noted that Avastin is not yet available for use (a Genentech statement said it is "discussing plans" to file for FDA approval) and it isn't a cure.

"The best cure for colon cancer is not to get it," Brooks said, "so we need to be focusing on early screening to prevent it, or detect it early."

Screening can help detect colon growths called polyps before they become cancerous. With early detection, Brooks said, five-year survival of colon cancer exceeds 90%; once the disease is advanced, however, five-year survival is only about 10%. Because early colon cancer has few symptoms, only about one-third of cases are detected at this stage.

Colorectal cancer is the third most common cancer in the United States and the second leading cause of cancer deaths. The American Cancer Society estimates that more than 147,000 people will be diagnosed with it this year, and about 57,000 will die from it.

Choking the Tumor

Avastin works against colon cancer by blocking a protein called vascular endothelial growth factor (VEGF). Tumors need the protein to grow and maintain their blood vessels. When VEGF is blocked, the tumor gets less blood, so it shrinks or spreads more slowly.

Several other drugs have tried to attack cancer by choking the tumor's blood supply, but Avastin appears to be the first one that actually has succeeded, researchers said.

Scientists are hopeful that blocking VEGF can help treat other types of cancer, too. Genetech is studying Avastin for use against kidney cancer, lung cancer, and breast cancer, though initial results of a breast cancer trial were disappointing.

Results from other studies of Avastin for colorectal cancer are also expected soon.

"We want to recognize the contributions of the numerous investigators and the courage of the hundreds of patients who participated (in the clinical trials)," Genentech's chief medical officer Susan Hellmann, MD, said in a statement.

J Cancer Res Clin Oncol (1999) 125:336–342

ORIGINAL PAPER

Jean-Marc Schlaeppi · Gerhard Siemeister
Karin Weindel · Christian Schnell · Jeanette Wood

Characterization of a new potent, in vivo neutralizing monoclonal antibody to human vascular endothelial growth factor

Received: 11 November 1998 / Accepted: 16 December 1998

Abstract Vascular endothelial growth factor (VEGF) is an important mediator of tumor-induced angiogenesis and represents a potential target for anticancer therapy. Therefore, we prepared a panel of monoclonal antibodies (mAb) against both the $VEGF_{121}$ and $VEGF_{165}$ isoforms. Three of them completely neutralized the mitogenic stimulation by VEGF of human umbilical vein endothelial cells at mAb concentrations below 0.1 μg/ml. The most potent one, with a dissociation constant (K_d) of 8 pM, inhibited, in a dose-dependent manner, VEGF-induced angiogenesis in a growth factor implant model in mice. A complete inhibition of the angiogenic response was obtained by daily intraperitoneal injections of 10 μg mAb/mouse. Angiogenesis induced by basic fibroblast growth factor was not inhibited by the mAb. Epitope mapping of the mAb, performed by competitive enzyme-linked immunosorbent assay and Western blot analysis, showed that it did not bind to the reduced and denatured monomer of VEGF. Substitutions of three residues (Q87R, G88K, Q89K), located on the major surface loop β5 to β6 of VEGF, resulted in the complete loss of binding (more than 400-fold reduction). The results suggest that the mAb binds primarily to a conformation-dependent epitope on the VEGF dimeric form, encompassing one of the loop regions involved in KDR receptor binding. The mAb with its strong neutralizing properties represents a useful agent for effective blocking of VEGF-mediated tumor neovascularization.

Key words VEGF · Neutralizing antibody · Epitope · Angiogenesis

Abbreviations *VEGF* vascular endothelial growth factor · *PDGF* platelet-derived growth factor · *bFGF* basic fibroblast growth factor · *KLH* keyhole limpet hemocyanin · *PBS* phosphate-buffered saline · *pAb* polyclonal antibody · *HUVE* human umbilical vein endothelial · *KDR* kinase domain receptor

Introduction

Angiogenesis, the sprouting of new capillaries from pre-existing blood vessels, is essential in reproduction, development and tissue repair. The process is tightly regulated by many factors, and deregulation leads to several pathophysiological condition such as cancer, rheumatoid arthritis, psoriasis, diabetic retinopathy and impaired healing (Folkman and Shing 1992; Folkman 1995). In particular, the growth of tumors beyond a certain size is dependent on angiogenesis (Folkman 1992) and clinical studies have shown that the intensity of the angiogenic response, measured by the degree of tumor micro-vascularization, correlated with poor prognosis in several types of cancer (Weidner 1993). Vascular endothelial growth factor (VEGF), also known as vascular permeability factor, appears as a unique and potent multifunctional cytokine, inducing both vascular permeability and angiogenesis in vivo (Ferrara et al. 1992; Dvorak et al. 1995; Ferrara and Davis-Smyth 1997). VEGF is a disulfide-linked dimeric glycoprotein, with homology to platelet-derived growth factor (PDGF) and placenta growth factor (Maglione et al. 1991). Recently, three additional members of the VEGF family were identified and designated VEGF-B, VEGF-C, and VEGF-D (Achen et al. 1998). There are at least four isoforms of VEGF that are generated by alternative

J.-M. Schlaeppi · C. Schnell · J. Wood
Novartis Pharmaceuticals,
Core Technology and Oncology Departments,
Novartis Limited, CH-4002 Basel, Switzerland

G. Siemeister[1] · K. Weindel
Institute of Molecular Medicine, Tumor Biology Center,
Freiburg, Germany

J.-M. Schlaeppi (✉)
Novartis Pharma AG, Bdg. K-681.2.44, CH-4002 Basel,
Switzerland
Tel.: +41-61-696-8091; Fax: +41-61-696-9301
e-mail: jean-marc.schlaeppi@pharma.novartis.com

Present address
[1] Schering AG, Experimentelle Onkologie, D-13342 Berlin

splicing of a single gene (Tischer et al. 1991). Many different cell types are able to produce VEGF but its mitogenic activity is restricted primarily to endothelial cells by way of two structurally related PDGF-receptor-like tyrosine kinases, Flt-1 and Flk-1/KDR, that are expressed predominantly on vascular endothelium (De Vries et al. 1992; Terman et al. 1992). These findings are consistent with the hypothesis that VEGF is primarily a paracrine mediator. Elevated VEGF expression has been reported in the vast majority of human tumors so far examined and VEGF overexpression has been associated with poor prognosis. Indeed, VEGF-rich tumors correlate with low survival rates in ovarian, gastric, lung and breast cancer patients (Paley et al. 1997; Maeda et al. 1996; Volm et al. 1997; Toi et al. 1995; Eppenberger et al. 1998; Linderholm et al. 1998). A direct role of VEGF in tumorigenesis has been clearly demonstrated in vivo by various means. Treatment with either VEGF-neutralizing monoclonal antibodies (Kim et al. 1993; Asano et al. 1995; Borgström et al. 1996), or antisense VEGF (Saleh et al. 1996) strongly inhibited the growth of tumours transplanted in nude mice. Inhibition of endogenous expression of VEGF leads to reduced tumorigenicity (Cheng et al. 1996). A retrovirus-mediated expression of a dominant-negative Flk-1 mutant, which interfered with the wild-type receptor-mediated signal transduction, suppressed tumor growth (Millauer et al. 1994). Embryonic stem cells with a disrupted VEGF gene ($VEGF^{-/-}$), exhibited reduced ability to form tumors in nude mice (Ferrara et al. 1996).

VEGF belongs to the cystine-knot family of growth factors. The recent resolution of the crystal structure of VEGF confirmed the overall resemblance between the VEGF monomer topology and that of PDGF, consisting of a central antiparallel four-stranded β sheet with the characteristic cystine knot at one end, and three solvent-accessible loop regions (Muller et al. 1977a, b). The identification of VEGF determinants involved in KDR/Flk-1 binding was determined by charge-reversal and alanine scanning mutagenesis (Muller et al. 1997 a; Keyt et al. 1996). Each functional KDR binding site consisted of two "hot spots" composed of binding determinants that were contributed by both subunits in the homodimer. The crystal structure of the complex between VEGF and the second domain of Flt-1 revealed that altogether 21 ligand residues contributed to the VEGF/receptor interface (Wiesmann et al. 1997). In the present study, we describe a new highly potent in vivo neutralizing anti-VEGF monoclonal antibody (mAb). Epitope analysis using VEGF mutants revealed that the mAb binds to one of the surface loops involved in receptor binding.

Materials and methods

Regents

Human recombinant $VEGF_{121}$ and $VEGF_{165}$ were kindly provided by Dr. G. Martiny-Baron (Institute of Molecular Medicine, Tumor Biology Center, Freiburg, Germany). They were produced in Sf9 insect cells infected with a recombinant baculovirus expressing the respective VEGF cDNA as described previously (Fiebich et al. 1993). Mutants of $VEGF_{3-121}$, with an amino-terminal His_6 tag, were prepared in *Escherichia coli* as described previously (Siemeister et al. 1998a, b). The proteins were refolded from inclusion-body material and purified by Ni^{2+}-affinity chromatography. Protein concentrations were measured by the Bradford protein assay using bovine serum albumin as a standard, and were confirmed by scanning analysis of sodium dodecyl sulfate (SDS)/polyacrylamide gels. Besides truncation of the N and C terminus, three loop regions designated (L-I, L-II, L-III) were subjected to site-directed mutagenesis. These surface loops were predicted from a model of VEGF based on the crystal structure of PDGF-B and corresponded to the segments connecting strands β1 to β3, β3 to β4, and β5 to β6 of the recently published VEGF crystal structure (Muller et al. 1997a). Within these loops, the VEGF residues were substituted with the corresponding residues from PDGF, which were selected to avoid disturbance of the overall structure of the VEGF mutant proteins. The VEGF mutants were characterized by competitive binding assays, SDS gel electrophoresis in non-reduced conditions, and for their stimulation of DNA synthesis in human umbilical vein endothelial (HUVE) cells (Siemeister et al. 1998a, b).

Antibody preparation and characterization

Two panels of anti-VEGF antibodies were prepared. The first one, described previously (Schlaeppi et al. 1996), consisted of four mAb and one polyclonal antibody (pAb 85618) generated by immunizing BALB/c mice and Chinchilla rabbits with human $VEGF_{121}$ conjugated to keyhole limpet hemocyanin (KLH). In addition, an antibody (pAb 85568) was generated against a synthetic peptide corresponding to the VEGF N-terminal sequence 1–26, common to all VEGF isoforms. The pAb was purified on a VEGF-peptide-bound thiopropyl-Sepharose column (Schlaeppi et al. 1996). A second panel of three mAb was prepared against $VEGF_{165}$. As for the smaller isoform, carbodiimide was used to couple recombinant human $VEGF_{165}$ to KLH. The mAb class and subclass were determined with an enzyme-linked immunosorbent assay (ELISA) isotyping kit from Bio-Rad Laboratories (Hercules, Calif.). The mAb were purified from hybridoma cell supernatants by ammonium sulfate precipitation and protein-G–Sepharose chromatography as described previously (Schlaeppi et al. 1996). For the mAb 4301-42-35 tested in vivo, the supernatant of cells grown in mini-PERM production modules (Heraeus Instruments, Osterode, Germany) was purified by protein-G–Sepharose chromatography. The purity of the mAb was assessed by SDS gel electrophoresis and the concentration was determined by absorbance at 280 nm. The characteristics of the mAb, namely their dissociation constants of the antigen/antibody equilibrium (K_d), and their cross-reactivity patterns, were determined by competitive ELISA as described previously (Schlaeppi et al. 1996). Briefly, purified mAb were incubated overnight at 4°C with increasing concentrations of $VEGF_{165}$ standards or analogs. The antibody/antigen mixture was then transferred to $VEGF_{165}$-coated microtiter plates (0.01 µg/well). After 1 h incubation at room temperature, binding of the antibody to the well was revealed by the addition of goat anti-(mouse Ig) antibody conjugated to alkaline phosphatase, followed by substrate addition and A_{405} measurement. The data were processed, using the Softmax 2.31 software (Molecular Devices, Menlo Oaks, Calif.) and four-parameter logistic curve fitting. The K_d was calculated as described previously (Schlaeppi et al. 1996).

Kinetic analysis by BIAcore technology

The molecular interactions between VEGF and mAb 4301-42-35 were measured by surface plasmon-resonance detection, using the BIAcore 2000 system as described previously (Karlsson and Fält 1997). Biotinylated mAb 4301-42-35 was diluted in HBS buffer (0.01 M HEPES pH 7.4, 0.15 M NaCl, 3 mM EDTA, 0.005% surfactant P20) to 50 µg/ml and injected at a flow rate of 5 µl/min

for 6 min over the surface of a streptavidin-coated sensor chip (Biacore, Uppsala, Sweden) according to the manufacturer's instruction. The amount of biotinylated mAb immobilized on the streptavidin-coated sensor chip corresponded to an average of 4800 resonance units. A biotinylated mouse mAb of the same isotype was immobilized as a control for unspecific binding and bulk refractive-index contributions. VEGF binding assays were performed at 37°C. $VEGF_{165}$, at concentrations ranging from 6.5 nM to 288 nM, was injected for 3 min at a flow rate of 10 µl/min. The dissociation of bound antigen in HBS buffer was followed for 6000 s at the same flow rate. The mAb surface was regenerated by injecting 10 µl 40 mM glycine/HCl pH 2.5. The association and dissociation rate constants (k_{on} and k_{off}) and the equilibrium dissociation constants ($K_d = k_{off}/k_{on}$) were determined using the BIAevaluation software version 3.0 with algorithms for global analysis, as described previously (Karlsson and Fält 1997).

Measurement of antibody-neutralizing activity in vitro

The neutralization of the VEGF mitogenic activity by anti-VEGF antibodies was measured on HUVE cells stimulated for 18 h with 5 ng/ml $VEGF_{165}$ in the presence of increasing concentrations of mAb. Then [*methyl*-^{3}H]thymidine was added and the incorporation was measured after a 6-h incubation as described previously (Fiebich et al. 1993).

Effects of VEGF-neutralizing antibody on VEGF-induced angiogenesis in vivo

The effects of mAb 4301-42-35 on the angiogenic response induced by VEGF and basic fibroblast growth factor (bFGF) were evaluated in a growth-factor implant model. A porous Teflon chamber (volume 0.5 ml) was filled with 0.8% agar containing heparin (20 U/ml) with or without human VEGF (3 µg/ml) or bFGF (0.3 µg/ml), and was implanted subcutaneously on the dorsal flank of female C57BL/6 mice. The mice, weighting 17–20 g, were obtained from the Novartis animal breeding facility and were kept in groups according to Swiss federal guidelines (six animals per treatment group). The treatment with mAb or vehicle (0.9% NaCl) was started 1 day before implantation of the chamber and continued for 5 days after. The mice were killed and the chambers removed after 5 days. In the first experiment, mAb 4301-42-35 was tested i.p. in daily doses of 2, 10 and 20 µg/mouse against VEGF only. In the second experiment a daily dose of 20 µg mAb/mouse was tested against both VEGF and bFGF. The vascularized tissue growing around the chamber was carefully removed weighed and the blood content assessed by measuring the hemoglobin content of the tissue. Hemoglobin was measured by the Drabkins method (Sigma Chemie GmbH, Deisenhofen, Germany). The significance of the differences between mAb- and vehicle-treated groups were analyzed by the non-parametric Kruskal-Wallis test.

Results

Preparation and in vitro characterization of anti-VEGF mAb

Seven monoclonal antibodies were obtained against VEGF by immunizing mice with protein conjugates made of either human recombinant $VEGF_{121}$ or $VEGF_{165}$. They were characterized by competitive ELISA, Western blot analysis and in vitro neutralizing activity on VEGF-stimulated HUVE cells. Their dissociation constants (K_d), measured by competitive ELISA, ranged from 0.01 nM to 1.93 nM $VEGF_{165}$. Double-mAb competitive-binding ELISA revealed that all the mAb were binding to overlapping epitopes on VEGF (data not shown). Three mAb neutralized the VEGF stimulation of DNA synthesis in HUVE cells by 100% at mAb concentrations below 0.1 µg/ml (Fig. 1). Among them, mAb 4301-42-35 (K_d = 8 pM/IgG_1) was the most potent, and fully inhibited the VEGF stimulation at equimolar concentration of binding sites, whereas the two others, mAb 4299-93-1 (K_d = 63 pM/IgG_{2a}) and mAb 4301-27-2 (K_d = 59 pM/IgG_{2a}), with lower affinity for VEGF, showed less potent neutralizing activity. Therefore, mAb 4301-42-35 was selected for further in vivo studies and detailed epitope analysis. By competitive ELISA, the mAb prepared with the KLH-$VEGF_{165}$ conjugate showed almost comparable binding affinity for both $VEGF_{165}$ and $VEGF_{121}$ (Table 1). Addition of up to 1 µg/ml placenta growth factor or PDGF-B to the mAb did not reduce the ELISA signal in the competitive assay, indicating that the mAb showed no cross-reactivity with these growth factors, despite their shared homology with VEGF. The kinetic analysis of the binding of $VEGF_{165}$ to immobilized mAb 4301-42-35 was determined with a BIAcore analyzer. As shown in Table 2, the apparent dissociation constant ($K_d = k_{off}/k_{on}$) was 20 pM. This value was close to the affinity constant measured in solution by competitive ELISA, and confirmed by another test system the high affinity of the mAb for VEGF. As shown in Fig. 2, Western blot analysis revealed that mAb 4301-42-35 was not binding to the reduced and denatured monomers of either $VEGF_{165}$ or $VEGF_{121}$, in contrast to a control anti-peptide antibody. Moreover, deletion of 17 residues of the N-terminal domain of VEGF ($VEGF_{18-121}$), which prevented dimer formation and thus resulted in a monomeric form of VEGF (Siemeister et al. 1998b), reduced the mAb binding by almost 50-fold, as shown

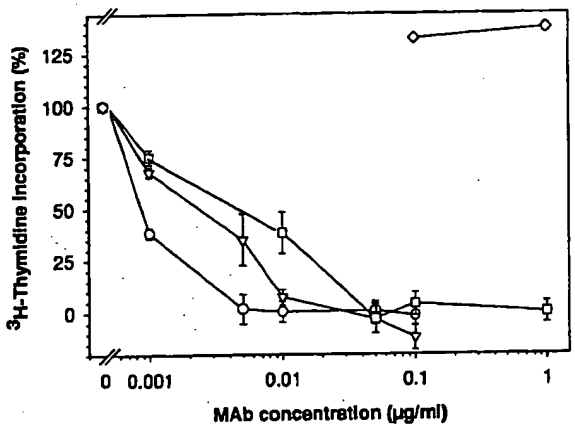

Fig. 1 The effects of anti-(vascular endothelial growth factor) (anti-VEGF) and control mAb on the growth of human umbilical vein endothelial (HUVE) cells stimulated by VEGF. HUVE cells were cultured for 18 h with 5 ng/ml $VEGF_{165}$ in the presence of increasing concentration of mAb. The growth of HUVE cells was measured by the incorporation of [*methyl*-^{3}H]thymidine during 6 h. ○ mAb 4301-42-35, ▽ mAb 4301-27-2, □ mAb 4299-93-1, ◇ control mAb (IgG_1)

Table 1 Structure and binding properties of the human vascular endothelial growth factor (VEGF) mutants to KDR and to mAb 4301-42-35. The structure was measured by sodium dodecyl sulfate gel electrophoresis under non-reducing conditions. KDR binding was measured by competitive binding assays on KDR-coated microtiter plates (+ +, binding wild type as; +, 2- to 20-fold lower; −, > 20-fold lower). Mitogenic activity is the stimulation of DNA synthesis measured by [$^3H_4$]thymidine incorporation (+ +, as wild type, +, 2- to 20-fold lower; −, > 20 fold lower). K_d was measured by competitive enzyme-linked immunosorbent assay. *HUVE* human umbilical vein endothelial cells

VEGF	Mutations	VEGF structure	Binding to KDR	Mitogenic activity on HUVE cells	mAb K_d (pM)
$VEGF_{1-165}$	Wild type	Dimeric	+ +	+ +	8
$VEGF_{1-121}$	Wild type	Dimeric	+ +	+ +	10
$VEGF_{18-121}$	N-terminal deletion (Δ1–17)	Monomeric	−	−	472
$VEGF_{3-110}$	C-terminal deletion (Δ111–121)	Dimeric	+	+	16
$VEGF_{3-121}$ L-I	D41N, E42Q, E44N, Y45F	Dimeric	+ +	+ +	11
$VEGE_{3-121}$ L-II	D63T, E64S, G65S, L66V	Dimeric	+	+	15
$VEGF_{3-121}$ L-III	R82E, K84E, Q87R, G88K, Q89K	Dimeric	−	−	> 4000
$VEGF_{3-121}$ L-IIIA	Q87R, G88K, Q89K	Dimeric	+	+	> 4000
$VEGF_{3-121}$ L-IIIB	R82E, K84E	Dimeric	−	−	16

Table 2 Kinetic parameters of VEGF binding to mAb 4301-42-35. $VEGF_{165}$, at concentrations ranging from 6.5 nM to 288 nM, was injected over a streptavidin-coated sensor chip surface containing around 4800 resonance units of mAb 4301-42-35. The kinetic constants (k_{on} and k_{off}) and the derived equilibrium dissociation constant ($K_d = k_{off}/k_{on}$) were determined with a BIAcore analyzer as described in Materials and methods

Parameter	
k_{on} ($M^{-1}s^{-1}$), mean ± SE	$4.4 \times 10^5 \pm 2 \times 10^2$
k_{off} (s^{-1}), mean ± SE	$9.0 \times 10^{-6} \pm 2.2 \times 10^{-8}$
K_d (M)	2.0×10^{-11}

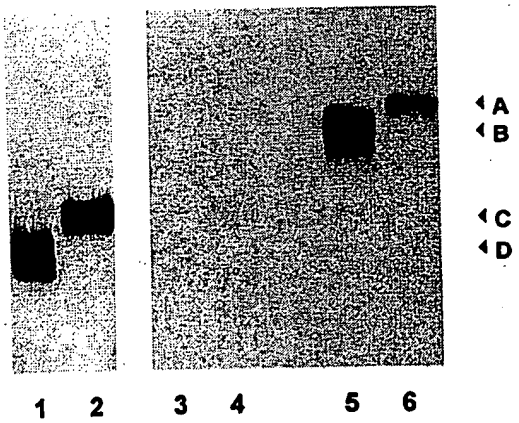

Fig. 2 Western blot analysis of antibody binding to VEGF dimer and monomer. Purified recombinant VEGF produced in Sf9 insect cells (0.15 μg/lane) was used for sodium dodecyl sulfate/polyacrylamide gel electrophoresis on 13% gel. $VEGF_{165}/VEGF_{121}$ momomer and $VEGF_{165}/VEGF_{121}$ dimer were obtained by running the gel electrophoresis in reducing (*lanes 1–4*) and nonreducing conditions (*lanes 5–6*) as described previously (Schlaeppi et al. 1996). *Lanes 1, 2* anti-$VEGF_{1-26}$ peptide pAb 85568; *lanes 3–6* mAb 4301-42-35. *A* $VEGF_{165}$ dimer (approx. 43 kDa), *B* $VEGF_{121}$ dimer (approx. 36 kDa), *C* $VEGF_{165}$ monomer (approx. 21.5 kDa), *D* $VEGF_{121}$ monomer (approx. 18 kDa)

by competitive ELISA (Table 1; Fig. 3A). The results indicate that the mAb recognized a conformation-dependent epitope on the VEGF homodimeric form. Truncation of the C-terminal domain ($VEGF_{110}$) by deletion mutagenesis showed almost no reduction of mAb binding (Table 1; Fig. 3A). Substitution of residues within the predicted surface loop III of VEGF (R82E, K84E, Q87R, G88K, Q89K) resulted in the complete loss of binding (more than 400-fold reduction), whereas substitutions within loop I and loop II had no effects on mAb binding (Table 1; Fig. 3A). As shown in Table 1, only three substitutions (Q87R, G88K, Q89K) in the loop-III mutant were responsible for the loss of binding of mAb 4301-42-35, as shown by the more than 400-fold reduction of binding to the mutant VEGF L-IIIA, whereas binding to the VEGF L-IIIB mutant with only two substitutions (R82E, K84E) was not reduced. These binding properties seemed to be unique to this mAb, since the other neutralizing mAb 4301-27-2 and mAb 4299-93-1 showed complete loss of binding to both VEGF L-IIIA and L-IIIB mutants in competitive (ELISA (K_d > 4 nM). These results indicate that, despite overlapping epitopes in the loop-III region, subtle differences in ligand binding could be observed between the three neutralizing mAb. Although all the mAb failed to bind to the VEGF L-III mutant by competitive ELISA, the rabbit pAb 85618 showed around 60% cross-reactivity with the loop-III mutant (Fig. 3B). The binding of the polyclonal antibody to VEGF L-III indicates that the amino acid substitutions introduced within the loop region were not causing a major disturbance of the overall structure of the VEGF mutant protein compared to that of the wild type.

Effects of anti-VEGF neutralizing antibody on VEGF-induced angiogenesis in vivo

The in vivo neutralizing activity of mAb 4301-42-35 was tested in a growth-factor-implant angiogenesis model in mice. In this animal model, the angiogenic response induced by VEGF or bFGF was measured by the increase in weight and blood content of tissue growing around the subcutaneously implanted chamber. As shown in

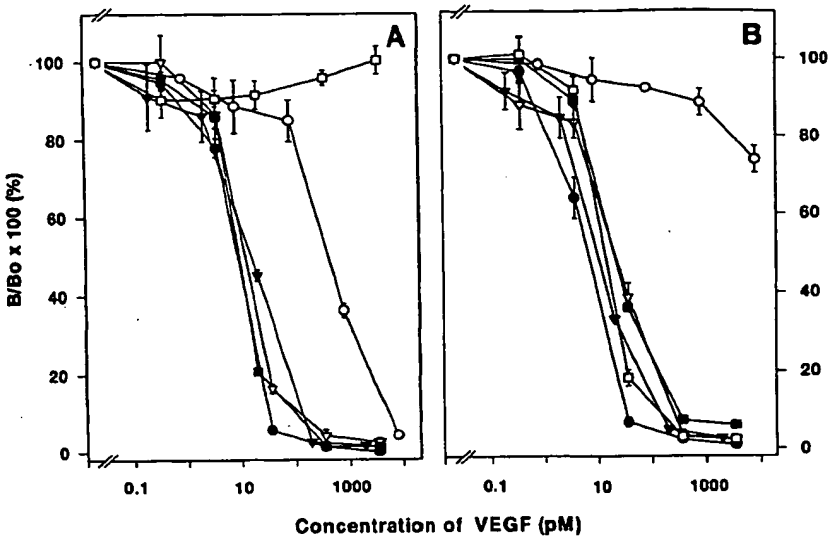

Fig. 3A,B Cross-reactivity analysis by competitive enzyme-linked immunosorbent assay. Binding of mAb 4301-42-35 (A) and pAb 85618 (B) to $VEGF_{121}$ and VEGF mutants. ● VEGF 121, ○ VEGF 18-121, ▼ VEGF 110, ▽ VEGF L-1, ■ VEGF L-II, □ VEGF L-III

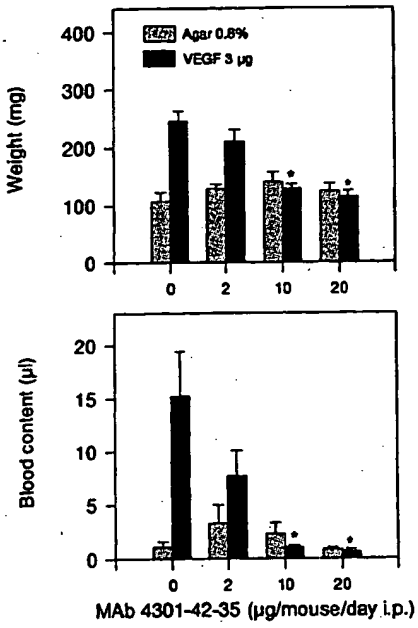

Fig. 4 In vivo neutralization of VEGF-induced angiogenesis by anti-VEGF mAb. Dose/response effects of daily i.p. injections of mAb 4301-42-35 (2, 10, 20 µg/mouse) on the weight and blood content of the tissue growing around a porous Teflon chamber containing VEGF (3 µg/ml) in 0.8% agar and heparin (20 U/ml) after subcutaneous implantation of the chamber for 5 days. Treatment with the mAb was started 1 day before implantation of the chambers and continued until the chamber was removed. Values are means ± SEM (n = 6), and are significantly different from those of the corresponding vehicle-treated group as indicated (*, $P < 0.05$)

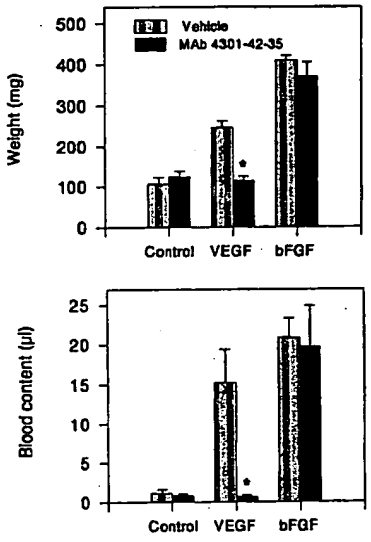

Fig. 5 In vivo neutralization of VEGF- but not basic-fibroblast-growth-factor(*bFGF*)-induced angiogenesis by anti-VEGF mAb. Effects of daily i.p. injections of mAb 4301-42-35 (20 µg/mouse) on the weight and blood content of the tissue growing around a porous Teflon chamber containing VEGF (3 µg/ml) or bFGF (0.3 µg/ml) in 0.8% agar and heparin (20 U/ml) after subcutaneous implantation of the chamber for 5 days. Treatment with the mAb was started 1 day before implantation of the chambers and continued until the chamber was removed. Values are means ± SEM (n = 6), and are significantly different from those of the corresponding vehicle-treated group as indicated (*, $P < 0.05$)

Fig. 4, daily intraperitoneal injections of the mAb inhibited the angiogenic response in a dose-dependent manner. A complete inhibition was observed with a daily dose of 10 µg mAb/mouse. In contrast, the angiogenic response induced by bFGF was not inhibited by the anti-VEGF mAb at daily dose of 20 µg mAb/mouse i.p. (Fig. 5).

Discussion

We used two protein conjugates, made of human $VEGF_{121}$ and $VEGF_{165}$, to generate a panel of high-affinity mAb. One of them (mAb 4301-42-35) showed a potent VEGF-neutralizing activity both in vitro and in vivo. The growth of HUVE cells stimulated by 5 ng/ml VEGF was effectively blocked by 0.01 µg/ml mAb, indicating that equimolar concentrations of mAb-bind-

ing sites were sufficient to block VEGF activity. The potent neutralizing activity of the mAb seemed to correlate with its high affinity for VEGF (K_d = 8 pM), since two other mAb with lower affinity were also less potent in the in vitro inhibition of HUVE cells. Other anti-$VEGF_{165}$ and anti-$VEGF_{121}$ neutralizing monoclonal antibodies have been described previously (Kim et al. 1992; Asano et al. 1998). A dissociation constant was reported only for mAb A4.6.1 (K_d = 0.8 nM) (Kim et al. 1992). Comparison of the neutralization activity of the different mAb on the growth of HUVE cells stimulated by VEGF reveals that the concentration of mAb 4301-42-35 needed to inhibit the growth of HUVE cells completely was between six to ten times lower than that needed with the other mAb, indicating that mAb 4301-42-35 corresponds to the most potent VEGF-neutralizing mAb described so far. In an in vivo model of growth-factor-induced angiogenesis, a daily injection of 10 μg mAb/mouse i.p. was sufficient to block the development of the angiogenic process induced by VEGF completely, but not that induced by bFGF. Compared to the in vitro experiments, a tenfold molar excess of mAb was necessary to block VEGF activity completely, which may account for the differences in bioavailability of the mAb. These results are in accordance with previous observations showing that VEGF is a potent angiogenic and vascular-permeability-enhancing factor, and represents a major positive effector of tumor neovascularization and growth (Kim et al. 1993; Saleh et al. 1996; Millauer et al. 1994). Epitope mapping of mAb 4301-42-35 revealed that the mAb was binding primarily to an epitope located on the solvent-accessible loop III of VEGF. Experimental evidence suggests that this loop, connecting the strands β5 to β6 of VEGF, is involved in VEGF receptor binding. Introduction of a glycosylation group at position 84 blocked VEGF binding to KDR (Keyt et al. 1996) and charge-reversal or alanine-scanning mutagenesis in this region showed that residues I83, K84 and P85 were critical for KDR binding (Muller et al. 1998a; Keyt et al. 1996). The crystal structure of the VEGF–$Flt\text{-}1_{D2}$-receptor complex confirmed that several residues of this loop were indeed buried in the interface (Wiesmann et al. 1997). It follows that the binding of mAb 4301-42-35 to this loop may explain its neutralizing activity. However, it may not result from a direct competition with receptor binding determinants since residues 87–89, critical for mAb binding, were not important for KDR binding, as shown by single alanine mutagenesis (Muller et al. 1997a; G. Siemeister and G. Martiny-Baron, unpublished observation). It is more likely that the tight binding of the mAb to the loop may produce steric hindrance or may hinder the concerted motion of loop β5 to β6, necessary for receptor binding. Indeed, although the epitopes of the other neutralizing antibodies, mAb 4299-93-1 and mAb 4301-27-2, encompassed residues directly involved in KDR binding, these mAb showed weaker neutralizing activity. Another property of mAb 4301-42-35 was its exclusive binding to the VEGF homodimeric form. The mAb showed no binding to reduced and denatured VEGF monomer and showed a 50-fold reduction of binding to the VEGF monomeric mutant ($VEGF_{18-121}$). These results suggest that both VEGF subunits contribute to the mAb binding. Since the three-dimensional structure of VEGF reveals that the N-terminal α helix of one monomer is associated with elements of loop regions of the other monomer (Muller et al. 1997a, b), we speculate that residues from the loop β5 to β6 of one monomer and residues from the N-terminal domain of the other contribute to the epitope of the mAb. Whether this unique combination accounts for the strong neutralizing activity of mAb 4301-42-35 compared to other anti-VEGF mAb remains open.

In conclusion, the new potent neutralizing monoclonal antibody described in this study represents a potential anticancer agent useful as an effective block of VEGF-mediated tumor neovascularization and tumor growth.

Acknowledgements We thank Prof. D. Marmé and Dr. G. Martiny-Baron (Institute of Molecular Medicine, Tumor Biology Center, Freiburg, Germany) for helpful discussion and H. Towbin for reading the manuscript. We thank S. Antz and A. Bordmann for technical assistance.

References

Achen MG, Jeltsch M, Kukk E, Makinen T, Vitali A, Wilks AF, Alitalo K, Stacker SA (1998) Vascular endothelial growth factor D (VEGF-D) is a ligand for the tyrosine kinases VEGF receptor 2 (Flk1) and VEGF receptor 3 (Flt 4). Proc Natl Acad Sci USA 95:548–553

Asano M, Yukita A, Matsumoto T, Kondo S, Suzuki H (1995) Inhibition of tumor growth and metastasis by immunoneutralizing monoclonal antibody to human vascular endothelial growth factor/vascular permeability $factor_{121}$. Cancer Res 55:5296–5301

Asano M, Yukita A, Matsumoto T, Hanatani M, Suzuki H (1998) An anti-human VEGF monoclonal antibody. MV833, that exhibits potent anti-tumor activity in vivo. Hybridoma 17:185–190

Borgström P, Hillan KJ, Srimararao P, Ferrara N (1996) Complete inhibition of angiogenesis and growth of microtumors by anti-vascular endothelial growth factor neutralizing antibody: novel concepts of angiostatic therapy from intravital videomicroscopy. Cancer Res 56:4032–4039

Cheng S-Y, Su Huang H-J, Nagane M, Ji X-D, Wang D, Shih CC-Y, Arap W, Huang CM, Cavenee WK (1996) Suppression of glioblastoma angiogenicity and tumorigenicity by inhibition of endogenous expression of vascular endothelial growth factor. Proc Natl Acad Sci USA 93:8502–8507

De Vries C, Escobedo JA, Ueno H, Houck K, Ferrara N, Williams LT (1992) The fms-like tyrosine kinase, a receptor for vascular endothelial growth factor. Science 255:989–991

Dvorak HF, Brown LF, Detmar M, Dvorak AM (1995) Vascular permeability factor/vascular endothelial growth factor, microvascular hyperpermeability, and angiogenesis. Am J Pathol 146:1029–1039

Eppenberger U, Kueng W, Schlaeppi J-M, Roesel JL, Benz C, Mueller H, Matter A, Zuber M, Luescher K, Litschgi M, Schmitt M, Foekens JA, Eppenberger-Castori S (1998) Markers of tumor angiogenesis and proteolysis (VEGF, uPA) independently define high- and low-risk subsets of node-negative breast cancer patients. J Clin Oncol 16:3129–3136

Ferrara N, Davis-Smyth T (1997) The biology of vascular endothelial growth factor. Endocrine Rev 18:4–25

Ferrara N, Houck K, Jakeman L, Leung DW (1992) Molecular and biological properties of the vascular endothelial growth factor family of proteins. Endocrine Rev 13:18–32

Ferrara N, Carver-Moore K, Chen H, Dowd M, Lu L, O'Shea KS, Powell-Braxton L, Hillan KJ, Moore MW (1996) Heterozygous embryonic lethality induced by targeted inactivation of the VEGF gene. Nature 380:439–442

Fiebich BL, Jäger B, Schöllmann C, Weindel K, Wilting J, Kochs G, Marmé D, Hug H, Weich HA (1993) Synthesis and assembly of functionally active human vascular endothelial growth factor homodimers in insect cells. Eur J Biochem 211:19–26

Folkman J (1992) The role of angiogenesis in tumor growth. Semin Cancer Biol 3:66–71

Folkman J (1995) Angiogenesis in cancer, vascular, rheumatoid and other disease, Nature Med 1:27–31

Folkman J, Shing Y (1992) Angiogenesis, J Biol Chem 267:10931–10934

Karlsson R, Fält A (1997) Experimental design for kinetic analysis of protein-protein interactions with surface plasmon resonance biosensors. J Immunol Methods 200:121–133

Keyt BA, Nguyen HV, Berleau LT, Duarte CM, Park J, Chen H, Ferrara N (1996) Identification of vascular endothelial growth factor determinants for binding KDR and FLT-1 receptors. Generation of receptor-selective VEGF variants by site-directed mutagenesis. J Biol Chem 271:5638–5646

Kim KJ, Li B, Houck K, Winer J, Ferrara N (1992) The vascular endothelial growth factor proteins: identification of biologically relevant regions by neutralizing monoclonal antibodies. Growth Factors 7:53–64

Kim KJ, Li B, Winer J, Armanini M, Gillett N, Phillips HS, Ferrara N (1993) Inhibition of vascular endothelial growth factor-induced angiogenesis suppresses tumour growth in vivo. Nature 362:841–844

Linderholm B, Tavelin B, Grankvist K, Henriksson R (1998) Vascular endothelial growth factor is of high prognostic value in node-negative breast carcinoma. J Clin Oncol 16:3121–3128

Maeda K, Chung Y-S, Ogawa Y, Takatsuka S, Kang S-M, Ogawa M, Sawada T, Sowa M (1996) Prognostic value of vascular endothelial growth factor expression in gastric carcinoma. Cancer 77:858–863

Maglione D, Guerriero V, Viglietto G, Delli-Bovi P, Persico MG (1991) Isolation of a human placenta cDNA coding for a protein related to the vascular permeability factor. Proc Natl Acad Sci USA 88:9267–9271

Millauer B, Shawver LK, Plate KH, Risau W, Ullrich A (1994) Glioblastoma growth inhibited in vivo by a dominant-negative Flk-1 mutant. Nature 367:576–578

Muller YA, Li B, Christinger HW, Wells JA, Cunningham BC, De Vos AM (1997a) Vascular endothelial growth factor: crystal structure and functional mapping of the kinase domain receptor binding site. Proc Natl Acad Sci USA 94:7192–7197

Muller YA, Christinger HW, Keyt BA, De Vos AM (1997b) The crystal structure of vascular endothelial growth factor (VEFG) to 1.93 Å resolution: multiple copy flexibility and receptor binding. Structure 5:1325–1338

Paley PJ, Staskus KA, Gebhard K, Mohanraj D, Twiggs LB, Carson LF, Ramakrishnan S (1997) Vascular endothelial growth factor expression in early stage ovarian carcinoma. Cancer 80:98–106

Saleh M, Stacker SA, Wilks AF (1996) Inhibition of growth of C6 glioma cells in vivo by expression of antisense vascular endothelial growth factor sequence. Cancer Res 56:393–401

Schlaeppi J-M, Eppenberger U, Martiny-Baron G, Küng W (1996) Chemiluminescence immunoassay for vascular endothelial growth factor (vascular permeability factor) in tumor-tissue homogenates. Clin Chem 42:1777–1784

Siemeister G, Schirner M, Reusch P, Barleon B, Marmé D, Martiny-Baron G (1998a) An antagonistic vascular endothelial growth factor (VEGF) variant inhibits VEGF-stimulated receptor autophosphorylation and proliferation of human endothelial cells. Proc Natl Acad Sci USA 95:4625–4629

Siemeister G, Marmé D, Martiny-Baron G (1998b) The alpha-helical domain near the amino-terminus is essential for dimerization of vascular endothelial growth factor. J Biol Chem 273:11115–11120

Terman BI, Dougher-Vermazen M, Carrion ME, Dimitrov D, Armellino DC, Gospodarowicz D, Böhlen P (1992) Identification of the KDR tyrosine kinase as a receptor for vascular endothelial cell growth factor. Biochem Biophys Res Commun 187:1579–1586

Tischer E, Mitchell R, Hartman T, Silva M, Gospodarowicz D, Fiddes JC, Abraham JA (1991) The human gene for vascular endothelial growth factor. Multiple protein forms are encoded through alternative exon splicing. J Biol Chem 266:11947–11954

Toi M, Inada K, Suzuki H, Tominaga T (1995) Tumor angiogenesis in breast cancer: its importance as a prognostic indicator and the association with vascular endothelial growth factor expression. Breast Cancer Res Treat 36:193–204

Volm M, Koomägi R, Mattern J (1997) Prognostic value of vascular endothelial growth factor and its receptor Flt-1 in squamous cell lung cancer. Int J Cancer 74:64–68

Weidner N (1993) Tumor angiogenesis: review of current applications in tumor prognostication. Semin Diagnost Path 10:302–313

Wiesmann C, Fuh G, Christinger HW, Eigenbrot C, Wells JA, De Vos AM (1997) Crystal structure at 1.7 Å resolution of VEGF in complex with domain 2 of the Flt-1 receptor. Cell 91:695–704